

Organic Anions. Part 11.¹ Hard Sphere Electrostatic Calculations on Group 1 Organometallic Compounds: Ion Pairs of Monoanions

Richard J. Bushby,* Helen L. Steel, and Myron P. Tytko
School of Chemistry, The University, Leeds, LS2 9JT

Structures for the lithium salts of allyl anion; W-, S-, and U-pentadienyl anion; benzyl anion; benzydryl anion; trityl anion; *trans,trans*-, *cis,trans*-, and *cis,cis*-1,3-diphenylallyl anion; cyclopentadienyl anion; indenyl anion; and fluorenyl anion have each been calculated by the HSE method and the results of these calculations have been compared with known X-ray crystal structures and the results of MO calculations. In almost all cases there is good agreement. In most cases HSE calculations, like MO calculations, find more than one potential bonding site for the cation and in such cases it may be that several species are in equilibrium in solution. Since the HSE method works satisfactorily for the lithium salts, R^- , Li^+ , it is then used to predict the structures of ion pairs, for this same series of anions, where the counterion is a caesium or there is a solvent-separated ion pair. R^- , Cs^+ ; R^- , SS^+ , and for the related triple ions, R^- , $2Li^+$; R^- , $2Cs^+$; R^- , $2SS^+$; R^- , Li^+ , Cs^+ ; and R^- , Li^+ , SS^+ (where SS^+ is the abbreviation used for the counterion in the solvent-separated ion pair and was modelled on Li^+ , 4THF, where THF = tetrahydrofuran). For the 1:1 ion pairs the predicted structure for the 'best' energy minimum is usually independent of the size of the counterion (Li^+ , Cs^+ , or SS^+) but the number of local minima decreases as the size of the counterion increases. The structures of triple ions, R^- , $2M^+$, cannot be inferred in any simple way from those of the 1:1 ion pairs, R^- , M^+ . The energy surfaces for these triple ions are rather flat, cation/cation repulsion is a very significant factor, and the structures vary widely according to the sizes of the counterions.

In applying the HSE model¹ to group 1 organometallic compounds it is assumed that bonding is wholly or almost wholly ionic. Whether or not this is a valid assumption has been the subject of a lively debate.^{2,3} Undoubtedly a major part of the problem has been that semi-empirical MO calculations and *ab initio* MO calculations using a small basis set exaggerate the degree of covalent bonding in group 1 organometallic compounds. *ab initio* MO calculations with large basis sets,⁴ on the other hand, suggest that the Me-Li bond is *ca.* 90% ionic, and that there is slightly less ionic character in the Me-Na bond but more ionic character in the bond to heavier group 1 metal ions. The argument over the degree of ionic character in these compounds cannot, however, be regarded as fully settled. One argument that has been used to support the 'covalent bonding' school of thought is that simple FMO theory⁵ or consideration of Möbius-Hückel aromatic character^{6,7} satisfactorily explains the structures of ion pairs of delocalised organic anions, for example the η^3 , bridged structure of allyllithium. It is also claimed that ionic/electrostatic arguments cannot explain these structures.⁵ What we show in this paper⁸ and in the paper that follows⁹ is that this claim is not true. A simple HSE model is just as good as FMO methods in rationalising these structures and the positions adopted by the counterions.

Model Systems.—Before considering the results of the HSE method for actual molecules it is helpful to consider what it predicts in simple model situations. The simplest 1:1 ion-pairing situation is that where a spherical anion is fixed in space and there is a single mobile cation. The cation will be attracted to the anion and will find its minimum-energy position when the two ions are in contact [Figure 1(a)]. The corresponding ion-pair surface¹ [Figure 1(b)] is a sphere whose radius is the sum of these of the anion and cation. All (η^1) points on this surface are equal in energy and the cation is free to move on the surface in any direction.

Another instructive model situation is one where the anion is composed of two spatially fixed, spherical negative atoms At1 and At2 which are in contact with each other [Figure 1(c)]. In this case the minimum-energy situation is one where the mobile cation adopts a bridging site. Actually there is a ring of such η^2 sites which are equienergetic. On a projection of the ion-pair surface [Figure 1(d)] this ring appears as a straight line A-B. It is easy to see why this is the minimum-energy situation. At any point on the surface to the left of the line A-B (η^1 sites where the cation only contacts At1) the attraction between the cation and At1 is the same. However, the closer the cation moves to the line A-B the greater the attraction to At2 becomes, reaching its maximum limiting value on the line itself.

A third instructive situation is one where the anion consists of three spatially fixed, spherical, negative atoms At1-At3 lying in contact with each other [Figure 1(e)]. In this case the minimum-energy site for a mobile cation is where it bridges all three atoms, point C on the projected ion-pair surface [Figure 1(f)]. Actually there are two of these η^3 sites which are equienergetic, one on the top and the other on the bottom of the molecule.

The model situations shown in Figure 1 are drawn for the simplest case where the radii of all of the atoms are the same and the charges ± 1 but the general form of these model ion-pair surfaces remains unaltered for all reasonable radii and regardless of the magnitudes of the charges (provided only that the signs remains unaltered). In actual molecular situations η^2 and η^3 sites analogous to those shown in Figures 1(d) and 1(f) are those encountered. In these molecules the cation does not, as is sometimes asserted, simply associate with the most negative atom. Instead it seeks bridging sites which may or may not include the most negative atom. In many cases there are several such bridging sites and a genuine 'ambident reactivity' problem ensues.¹⁰

The situation where a 'delocalised' anion is associated with two mobile cations is complex. Even for simple model anions [Figure 1(a), 1(c), 1(e)] the result is strongly dependent on

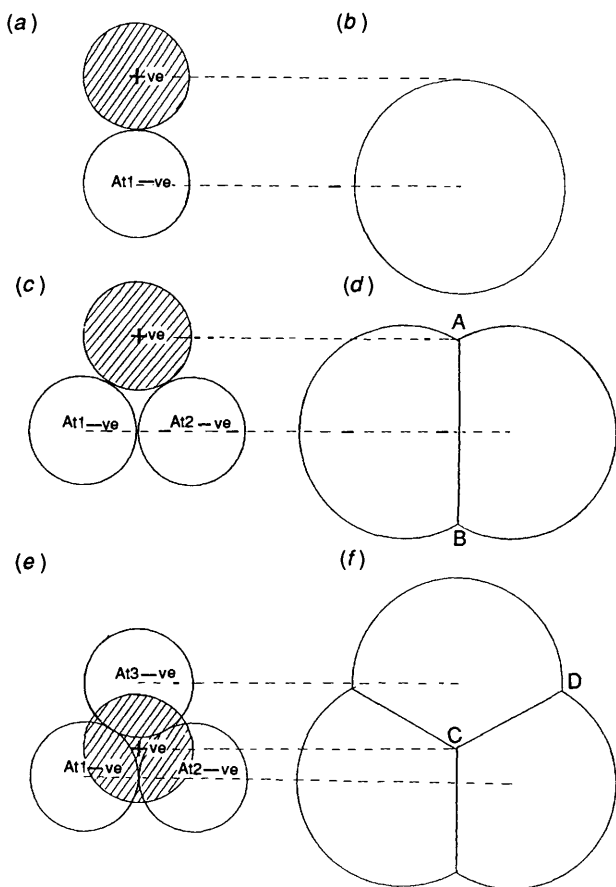
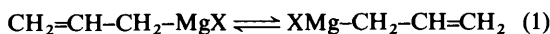


Figure 1. Simple model ion pairs (left) together with a projection of the corresponding ion-pair surfaces (right); the surfaces defined by the nucleus of the mobile cation as it rolls over the surface of the anion. An explanation of the labels and terms used is given in the text.

relative radii and charges of the atoms. The sites adopted by the two cations lie on the same ion-pair surface and sometimes, but not always, correspond to sites recognised in the monocation situation. For example, if one more cation is added to the cluster of atoms depicted in Figure 1(e) then a structure with one cation at the top point C and another at the site immediately below it, \bar{C} , may form but only if anion/cation attractive term is large relative to cation/cation repulsion. If cation/cation repulsion is larger then one of the cations is displaced into an η^2 site, for example along the line C–D. Each situation must be treated on its own merits.

The Allyl Anion.—Workers have speculated about the structure of the salts of this anion, particularly the lithium and magnesium salts, for many years. Early workers tended to assume that these were isostructural with propene; the Li or MgX being σ -bonded to a tetrahedral CH_2 (an η^1 complex). When it was shown by ^1H NMR spectroscopy that the two CH_2 groups in allyl Grignard were equivalent to each other it was assumed that there was a pair of rapidly equilibrating η^1 structures [equation (1)].¹¹



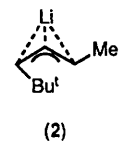
* The planar geometry (ref. 31) used for allyl in the HSE calculations was taken from A. S. Patterson, (Ph.D. Thesis, University of Leeds, 1977): C–C 1.385 Å; C–H 1.080 Å; $\angle(\text{C}-\text{C}-\text{C})$ 131.7°; $\angle(\text{H}-\text{C}-\text{H})$ 117.0°. Use of the Schleyer geometry (ref. 29) gives essentially the same results.

A similar interpretation was given to the ^1H NMR spectrum of allyl-lithium¹² but the results for both these systems could be explained equally well by a single structure with the metal ion symmetrically bridging two equivalent CH_2 groups (a π or η^3 complex). It is now known that allyl Grignard falls into the first category (η^1).^{13–17} Some doubt still remains over the structure of allyl-lithium although the monomer is probably symmetrical (η^3). Evidence supporting this structure, based on ^{13}C NMR isotopic perturbation,¹⁵ was advanced by Bywater¹⁸ and Schleyer.¹⁹ However, the same results were interpreted by Schlosser^{14,20} as evidence that allyl-lithium in THF is a rapidly equilibrating pair of *unsymmetrical* $\eta^3(\pi)$ complexes (i.e. an η^3 structure but with unequal Li– CH_2 bond lengths). Schleyer has recently suggested a solution to this problem²¹ based on the proposal that allyl-lithium in THF exists as a dimer, and calculations show that this would have the required unsymmetrical η^3 structure. This proposal is, however, contrary to some results from previous work on aggregation in THF.^{22,23}

Like the NMR studies, attempts to solve the problem by X-ray crystallography, have failed to clarify the situation.^{24–27} The allyl-lithium tetramethylethylenediamine complex proves to be an endless polymer in which each lithium bridges two allyl units.²⁴ Allyl-lithium pentamethyldiethylenetriamine complex,²⁵ the tetramethylethylenediamine complex of anion (1),²⁶ and the tetramethylethylenediamine complex of the anion (2)²⁷ all have unsymmetrical η^3 bridged structures with one Li– C_α bond being significantly shorter than the other. In each of these cases, however, the unsymmetrical nature of the system could be attributed to factors other than an intrinsic preference of allyl-lithiums for slightly unsymmetrical structures.



(1)



(2)

Many MO calculations support the view that allyl-lithium should be η^3 and symmetrical.^{28,29}

Experimental evidence for allylsodium,^{16,21,30} allylpotassium,^{14,20,21} and allylcaesium^{14,20} based on IR spectroscopy^{16,28} and on the ^{13}C NMR isotopic perturbation method^{14,15,20,21} unambiguously shows that these are symmetrical η^3 structures.

Figure 2(a) shows the ion-pair surface³¹ for allyl-lithium, Figure 2(b) that for allylcaesium, and the corresponding ion-pair surface for a solvent-separated ion pair is shown in Figure 2(c).* In each case the main HSE minima for a single counterion is found along the line A–B; i.e., positions where the counterion bridges the two terminal CH_2 groups. This is in agreement with most of the experimental evidence detailed above. In the case where HMO charges have been used there is an arc of equienergetic sites on the line A–B but when STO-3G *ab initio* MO charges are used the absolute minimum for the lithium salt is found at position A. In this case shallow local minima are also found at positions C₁ and C₂ [Figure 2(a)]. The ‘appearance’ of additional local minima when *ab initio* or semi-empirical MO charges are used instead of HMO charges is a common factor in all of these HSE calculations. It arises in part because CNDO-11 and STO-3G *ab initio* MO calculations, unlike HMO calculations, place some charge on the hydrogens so that sites in which bridging to these hydrogens occurs become a possibility. Such sites are invariably high in energy relative to the main minima and may not be significant. The way in which the major minima arise can be understood by reference to Figure 3. Figure 3(a) is similar to Figure 1(b) except that energy contours are

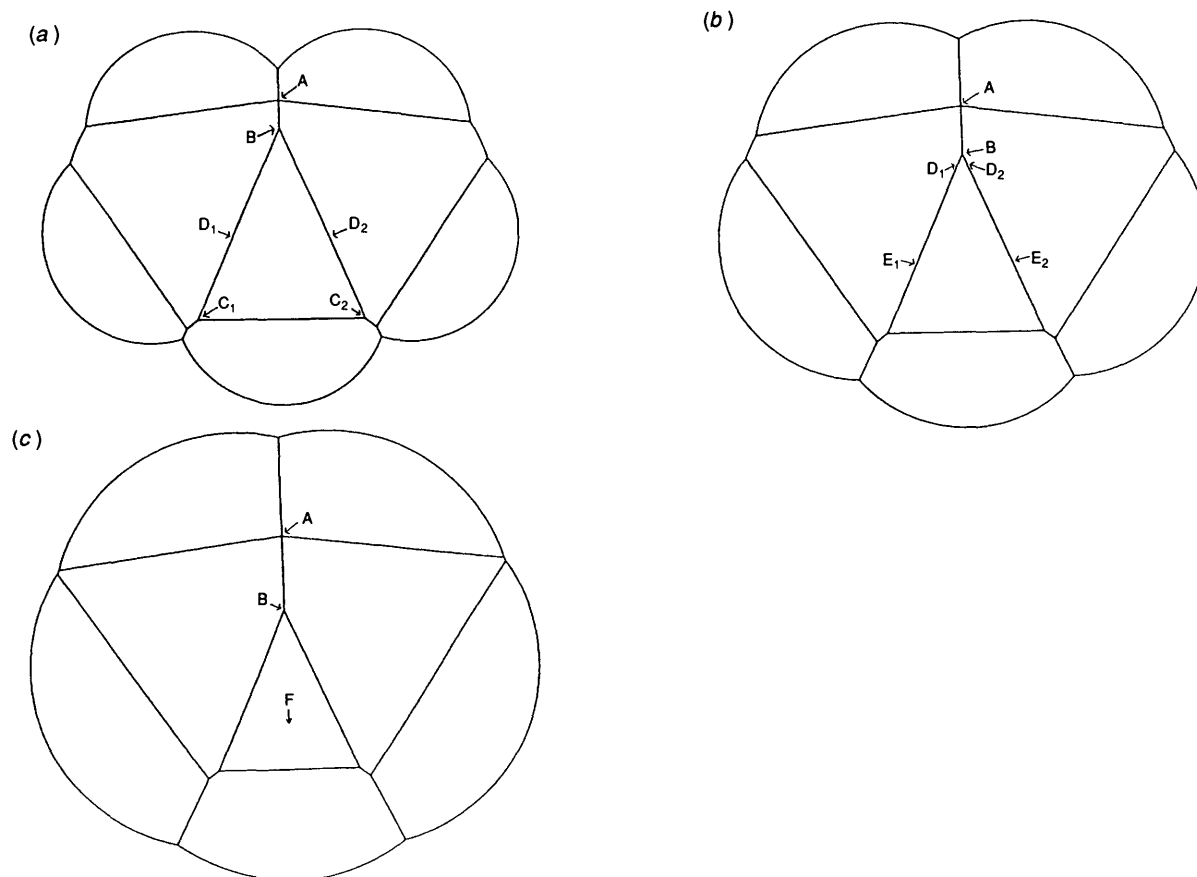


Figure 2. Ion-pair surfaces and associated HSE minima for the Li^+ , Cs^+ , and SS^+ ion pairs of allyl^- . (SS^+ is the abbreviation used for the counter-ion in a solvent-separated ion pair which was modelled on Li^+ , 4THF). The geometry of the anion was taken from A. S. Patterson (Ph.D. Thesis, University of Leeds, 1977). Since this geometry is planar top and bottom surfaces are equivalent and \bar{A} lies directly beneath A (a bar always indicates a point on the lower surface). Drawn strictly to scale the surface for allyl^- , SS^+ would be much larger than that for allyl^- , Li^+ but for convenience of representation the diagrams have been scaled to similar widths. The positions of the energy minima were determined by the automated x/y -search procedure and were all checked by inspection of suitably magnified contour plots or pair of contour plots (for the triple ions) as described in the last paper. For the simple 1:1 ion pairs it was shown that the same minima and local minima were found using a computer program based on an 'atom-by-atom' search of the energy surface (ref. 1 & M. P. Tytko, Ph.D. Thesis, University of Leeds, 1982). Energies are expressed in the form $E.e$ and are in kcal mol^{-1} (ref. 1). For a medium other than a vacuum they should be divided by the effective microscopic relative permittivity. Allyl^- , Li^+ [Figure 2(a)] (i) HMO charge distribution, minimum a line of equienergetic points from A to B, \bar{A} to \bar{B} , 146.3 ($E.e/\text{kcal mol}^{-1}$); no local minima. (ii) STO-3G *ab initio* MO charge distribution, minimum at A, \bar{A} , 143.8 (*i.e.* the minima with the lithium at A and \bar{A} are degenerate with an energy of $-143.8 \text{ kcal mol}^{-1}$); local minima at C₁, C₂, \bar{C}_1 , \bar{C}_2 , 121.4. Allyl^- , Cs^+ [Figure 2(b)] HMO charge distribution, minimum a line of equienergetic points from A to B, \bar{A} to \bar{B} , 98.0; no local minima. Allyl^- , SS^+ [Figure 2(c)] HMO charge distribution, minimum a line of equienergetic points from A to B, \bar{A} to \bar{B} , 53.6; no local minima. Allyl^- , 2Li^+ [Figure 2(a)] HMO charge distribution, minimum at B- \bar{D}_1 (*i.e.* on the top at point B and the underside at \bar{D}_1), B- \bar{D}_2 , B- \bar{D}_1 , B- \bar{D}_2 , 193.8; local minima not checked (*i.e.* such minima were found by the automated search procedure but not checked by inspection of contour diagrams). Allyl^- , 2Cs^+ [Figure 2(b)] HMO charge distribution, minimum at \bar{D}_1 - \bar{D}_2 , \bar{D}_1 - \bar{D}_2 , 139.4; local minima not checked. Allyl^- , 2SS^+ [Figure 2(c)] HMO charge distribution minimum at B- \bar{B} , 79.3; local minima not checked. Allyl^- , Li^+ , Cs^+ [Figures 2(a) and (b)] HMO charge distribution, minimum at B [(Figure 2(a))- \bar{E}_1 [(Figure 2(b))], B- \bar{E}_2 , B- \bar{E}_1 , B- \bar{E}_2 , 173.5; local minima not checked. Allyl^- , Li^+ , SS^+ [Figures 2(a) and (c)] HMO charge distribution, minimum at B [(Figure 2(a))- \bar{F} [(Figure 2(c))], B- \bar{F} , 156.9; local minima not checked. For the triple ions in which the two cations are different, say allyl^- , Li^+ , Cs^+ the surface described by the Li^+ nucleus is shown in Figure 2(a) and that by the Cs^+ in Figure 2(b). These two surfaces should be considered as being co-centred. The minimum B- \bar{E}_1 then represents a state with the lithium at B on the inner surface and the caesium at \bar{E}_1 on the outer.

shown. It is the HSE surface for an anion made up of two atoms of equal radius and charge ($-\frac{1}{2}$). The surface is symmetrical about an axis passing through the nuclei of the two atoms. In projection the paired rings of equienergetic contours appear as straight lines (for example a,b and a',b'). The ring of equienergetic positions corresponding to the energy minimum appears as the line A-B. The corresponding surface for allyl anion using HMO charges is shown in Figure 3(b). Within this it is clear that a segment of the energy surface, that involving the two charged atoms, remains the same. The length of the line

A-B is curtailed, however, by the surfaces of C-3 and two of the hydrogens. Since HMO places charge only on C-1 and C-3 the other atoms only affect the surface by virtue of volume exclusions. When STO-3G *ab initio* MO charges are used [Figure 3(c)], however, since all of the atoms are charged the symmetry of the surface is destroyed and positions along the line A-B are no longer equienergetic.

So far as the major minima are concerned the form of the energy surface is similar for allyl^- , Li^+ ; allyl^- , Cs^+ , and allyl^- , SS^+ . However, for the triple ions allyl^- , M_1^+ , M_2^+ * the predicted structures (given in Figure 2) are very dependent on the radii of the metal ions. Only in the case allyl^- , 2SS^+ is cation/cation repulsion negligible so that the cations occupy

* Throughout, M_1^+ , and M_2^+ refer to two separate cations; the subscripts are not multiplying subscripts.

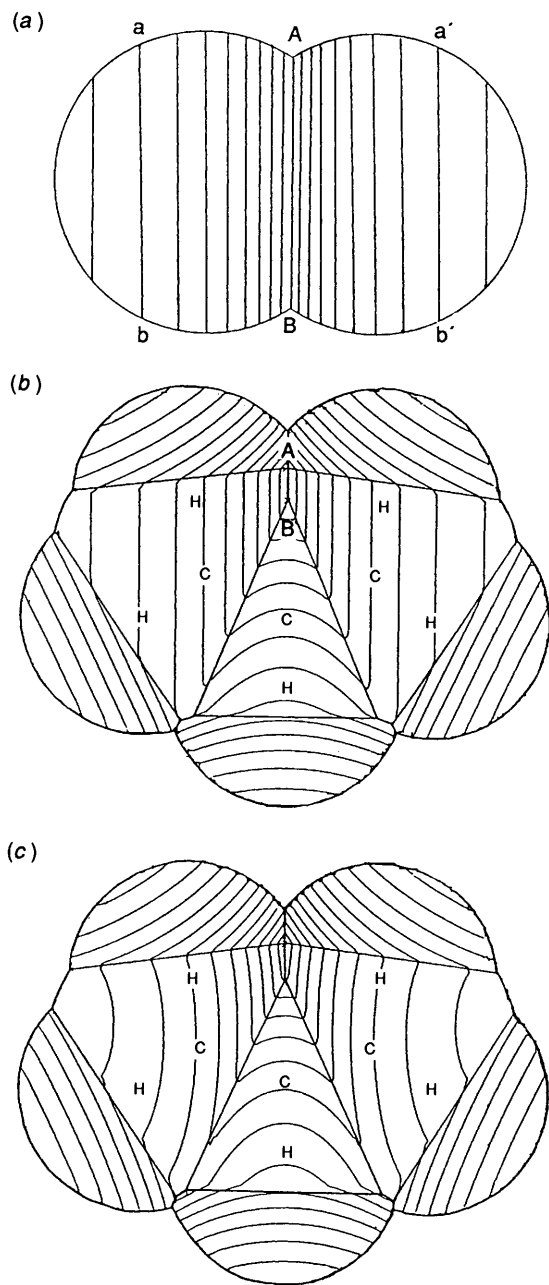
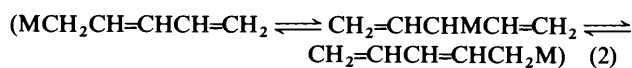


Figure 3. (a) Isoenergetic contours drawn on the ion-pair surface of an anion composed of two equally charged atoms [cf. Figure 1(a)]; (b) contours drawn on the ion-pair surface of the allyl anion, HMO charge distribution; (c) contours on the ion-pair surface of the allyl anion, STO-3G *ab initio* MO charge distribution.

sites analogous to those found in the 1:1 ion pair, allyl⁻, SS⁺, each one adopting a bridging site, one above and one below the plane of the anion [positions **B** and **B'** in Figure 2(c)]. When one or other of the cations is smaller, however, cation/cation repulsion displaces one of the cations from this simple arrangement. Some of the resultant structures are unsymmetrical; e.g., the dilithium salt [positions **B** and **D**₁ in Figure 2(a)], and some are symmetrical [e.g., the Li⁺, SS⁺ salt, Figures 2(a) and 2(c)].

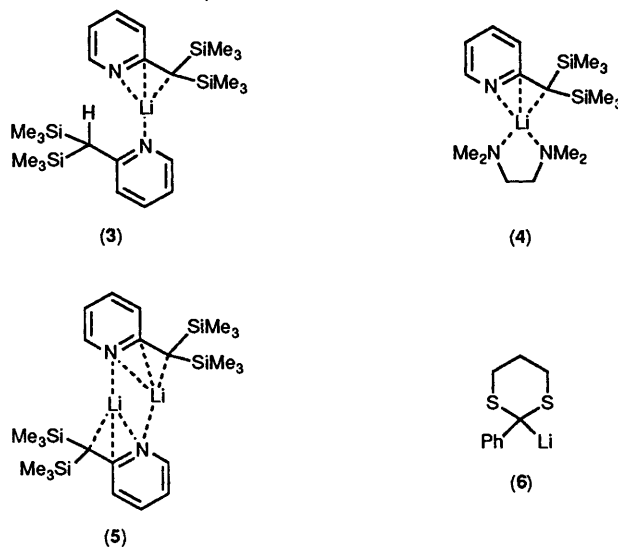
The Pentadienyl Anion.—The pentadienyl anion exists in three principle conformations; W-, sickle (or S)-, and U-shaped.^{32–34} Initial studies of the structure of metal ion salts assumed these to be a series of equilibrating σ-bonded (η¹) species³⁵ [equation (2)]. This is probably correct for the



beryllium, magnesium, and zinc salts.³⁶ For the group 1 metal salts the situation is complicated by aggregation³⁷ but it is normally assumed that in the monomeric ion pairs the cations adopt bridging positions analogous to that in allyl-lithium. This is supported by MO calculations on the W-, S-, and U-conformations of the lithium salt at the CNDO-II level^{6,38} and on the U-conformation of the potassium salt at the STO-3G level.³⁹ Although it may well be that there is some deviation from strict planarity of the pentadienyl systems, in response to the presence of the counterion,⁴⁰ for the HSE calculations we have used planar geometries for all three conformations. These were derived from CNDO-II MO calculations.⁶ The ion-pair surfaces for the Li⁺, Cs⁺, and SS⁺ ion pairs of the W-, S-, and U-conformations are shown in Figures 4–6. For the 1:1 Li⁺ salts the structures predicted are in accord with those predicted by MO methods, for W-pentadienyl-lithium [Figure 4(a), HMO or CNDO-II charges] the main minima bridge C-1/C-3 or C-3/C-5 with a local minimum in the C-2/C-3/C-4 bridging position. A similar pattern emerges for W-pentadienyl caesium but it is interesting to note that in the SS⁺ ion pair the central C-2/C-3/C-4 bridging site becomes the major minimum. For S-pentadienyl-lithium [(Figure 5(a)) the major minima found (at sites **A** and **B**) correspond to those predicted by MO methods.⁶ The HSE result for S-pentadienylcaesium is similar to that for the lithium salt but for the SS⁺ ion pair only one minimum [at **A**, Figure 5(c)] is obtained. For U-pentadienyl-lithium, -caesium, or solvent-separated ion pair a central minimum is predicted by HSE methods, a prediction which is in agreement with MO calculations. As in the case of the allyl anion, when CNDO-II charges rather than HMO charges are employed, additional high-energy local minima are predicted by the HSE method.

Also, as in the case for allyl anion, the situation for triple ions, pentadienyl⁻, M₁⁺, M₂⁺, is complicated and in the case of small cation the situation is normally dominated by cation/cation repulsion. Only in the case of U-pentadienyl⁻ (where the cation/anion attractive term is relatively large) do the cations in these triple ions always occupy similar sites to those found in the 1:1 ion pairs.

The Benzyl Anion.—The first single-crystal X-ray diffraction structure for a derivative of benzyl-lithium was that for {PhCH₂,



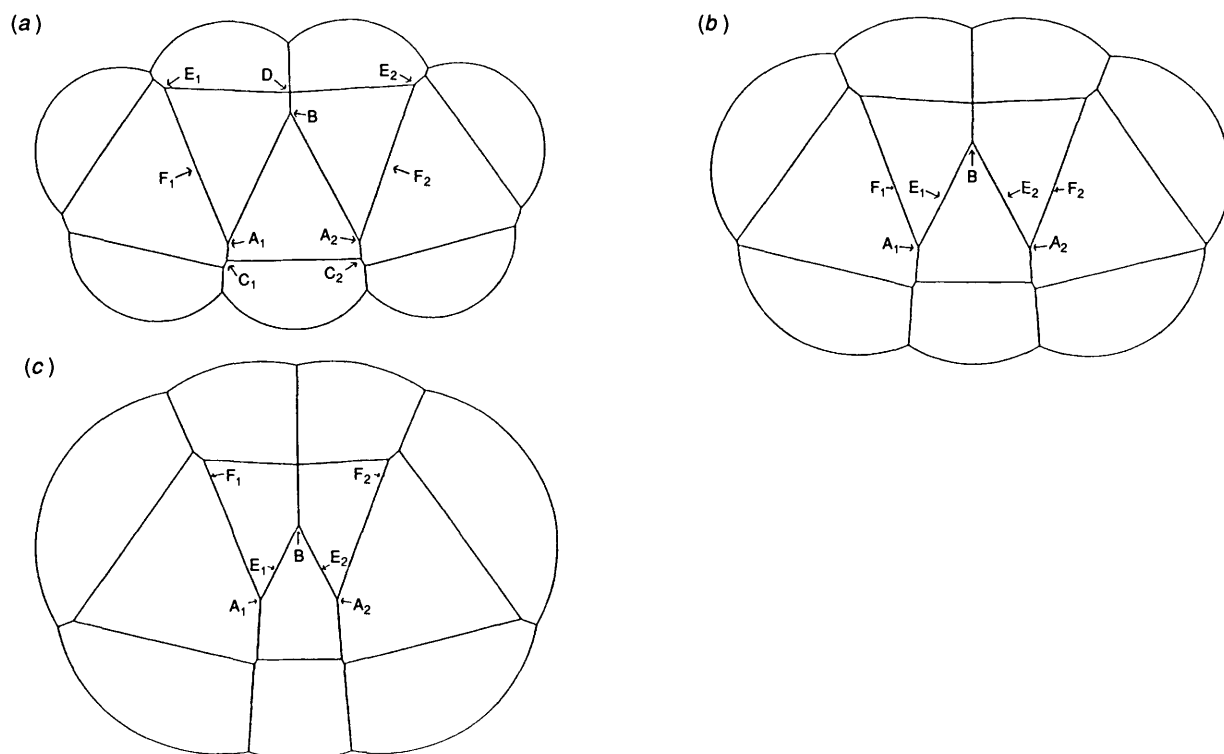


Figure 4. Ion-pair surfaces and associated HSE minima for the Li^+ , Cs^+ , and SS^+ ion pairs of W-pentadienyl^- . The terms used are defined in the headings to Figures 1 and 2. Since the anion is planar $\bar{\text{A}}_1$ lies directly below A_1 . W-pentadienyl^- , Li^+ [Figure 4(a)] (i) HMO charge distribution, minimum at A_1 , A_2 , $\bar{\text{A}}_1$, $\bar{\text{A}}_2$, 123.0; local minimum B , $\bar{\text{B}}$, 115.2; no further local minima. (ii) CNDO-II charge distribution, minima at C_1 , C_2 , $\bar{\text{C}}_1$, $\bar{\text{C}}_2$, 117.9; local minima at B , $\bar{\text{B}}$, D , $\bar{\text{D}}$, 108.3; E_1 , E_2 , $\bar{\text{E}}_1$, $\bar{\text{E}}_2$, 100.2; no further local minima. W-pentadienyl^- , Cs^+ [Figure 4(b)] HMO charge distribution, minimum at A_1 , A_2 , $\bar{\text{A}}_1$, $\bar{\text{A}}_2$, 87.3; local minima at B , $\bar{\text{B}}$, 85.7; no further local minima. W-pentadienyl^- , SS^+ [Figure 4(c)] HMO charge distribution, minimum at B , $\bar{\text{B}}$, 51.1; local minima at A_1 , A_2 , $\bar{\text{A}}_1$, $\bar{\text{A}}_2$, 51.0; no further local minima. W-pentadienyl^- , 2Li^+ [Figure 4(a)] HMO charge distribution, minimum at A_1 - $\bar{\text{F}}_2$, A_2 - $\bar{\text{F}}_1$, $\bar{\text{A}}_1$ - $\bar{\text{F}}_2$, $\bar{\text{A}}_2$ - $\bar{\text{F}}_1$, 166.9; local minima not checked. W-pentadienyl^- , 2Cs^+ [Figure 4(b)] HMO charge distribution, minimum at A_2 - $\bar{\text{E}}_1$, A_1 - $\bar{\text{E}}_2$, $\bar{\text{A}}_2$ - $\bar{\text{E}}_1$, $\bar{\text{A}}_1$ - $\bar{\text{E}}_2$, 123.3; local minima not checked. W-pentadienyl^- , 2SS^+ [Figure 4(c)] HMO charge distribution, minimum at E_1 - $\bar{\text{E}}_2$, E_2 - $\bar{\text{E}}_1$, 75.2; local minima not checked. W-pentadienyl , Li^+ , Cs^+ [Figures 4(a) and (b)] HMO charge distribution, minimum A_1 [Figure 4(a)]- $\bar{\text{F}}_2$ [Figure 4(b)], A_2 - $\bar{\text{F}}_1$, $\bar{\text{A}}_1$ - $\bar{\text{F}}_2$, $\bar{\text{A}}_2$ - $\bar{\text{F}}_1$, 149.1; local minima not checked. W-pentadienyl , Li^+ , SS^+ [Figures 4(a) and (c)] HMO charge distribution, minimum A_1 [Figure 4(a)]- $\bar{\text{F}}_2$ [Figure 4(c)], A_2 - $\bar{\text{F}}_1$, $\bar{\text{A}}_1$ - $\bar{\text{F}}_2$, $\bar{\text{A}}_2$ - $\bar{\text{F}}_1$, 133.9; local minima not checked.

Li , $\text{N}[\text{CH}_2\text{CH}_2]_3\text{N}$.⁴¹ In this the lithium is in an η^3 site bridging between the benzylic CH_2 carbon and an *ortho* carbon of the benzene ring [close to position $\bar{\text{D}}$ in Figure 7(a)]. The bidentate 1,8-diazabicyclo-octane (DABCO) ligand forms a bridge from one lithium to the next giving, in all, an 'infinite' chain. The η^3 site occupied by the cation is similar to that in allyl-lithium and, as in the allyl case, the cation induces deviations from planarity.^{41,42} This is confirmed by NMR studies of benzyl-lithium derivatives^{43,44} but similar NMR studies of the ion pairs of the heavier group 1 metals suggest that the benzylic moiety is planar.⁴⁴ An η^3 site similar to that found in Stucky's study was also found in the silylated benzyl-lithium $\{\text{Li}, \text{Me}_2\text{NCH}_2\text{CH}_2\text{NMe}_2\}_2\{[2-\text{CH}(\text{SiMe}_3)\text{C}_6\text{H}_4]_2\}$ ⁴⁵ and in several lithiated α -methylpyridines (3)–(5).⁴⁶ However, the diethyl ether complex of benzyl-lithium $\{\text{Li}, (\text{Et}_2\text{O})(\text{CH}_2\text{Ph})\}_\infty$ has a polymeric structure in which the lithium is η^2 coordinated to each benzyl anion *via* the benzylic carbon and the first carbon of the aromatic ring.⁴⁷ Each lithium, however, bridges two benzyl groups which makes comparisons difficult. Unique sites for the lithium are also found in the dithiane (6)⁴⁸ and in $\{[\text{Li}(\text{Me}_2\text{NCH}_2\text{CH}_2\text{NMe}_2)]_2\{(\text{Me}_2\text{NCH}_2\text{CH}_2\text{NMe}_2)\text{-Li}(\text{CH}_2\text{Ph})_2\}\{[\text{Mg}(\text{CH}_2\text{Ph})_2]\}$ ⁴⁹ Dilithium salts of the dianions from 1,8-naphthaquinodimethane,⁵⁰ *ortho*-,^{51,52} *meta*-,⁵³ and *para*-⁵⁴-quinodimethane and *ortho,ortho'*-dimethylenebiphenyl⁴⁵ can also be regarded as formal derivatives of benzyl-lithium and η^3 , α -carbon/*ortho*-carbon-bridged, sites occur in some of these^{50,52,53} but in others cation/cation repulsion

results in unique structures that from the HSE standpoint require separate treatment.

MO calculations also highlight the importance of η^3 , α -carbon/*ortho*-carbon-bridged, sites but Schleyer⁵⁵ claims that CNDO calculations on benzyl-lithium give the best energy minimum with the lithium almost over the centre of the benzene ring (η^6). This agrees with the report of Sygula and Rabideau⁵⁶ whose MNDO calculations give a minimum with the lithium over the benzene ring and local minima at the η^3 sites. Lipkowitz *et al.*,⁴² also using the MNDO method, only report a minimum at the η^3 site.

For the HSE calculations a non-planar benzyl anion geometry was used which was taken from Stucky's X-ray crystal structure.⁴¹ For benzyl-lithium the two types of minima highlighted by crystallographic and MO studies were found; η^3 sites in which the lithium bridges the α -carbon and an *ortho*-carbon [Figure 7(a); A , B , $\bar{\text{C}}$, $\bar{\text{D}}$] and η^6 sites with the lithium above or below the benzene ring [Figure 7(a); E , $\bar{\text{F}}$, $\bar{\text{G}}$, $\bar{\text{H}}$]. The balance between these two types of site for benzyl-lithium is seen to vary according to whether an HMO or STO-3G *ab initio* MO charge distribution is employed and as in direct MO calculations of benzyl-lithium the HSE calculations suggest quite a fine balance. For the larger counterions the situation appears to be very similar except that in the SS^+ case no minimum is found over the ring (HMO charges). For the ion triplets the two counterions seem always to prefer two of the η^3 (benzylic) sites, at least when an HMO charge distribution is employed.

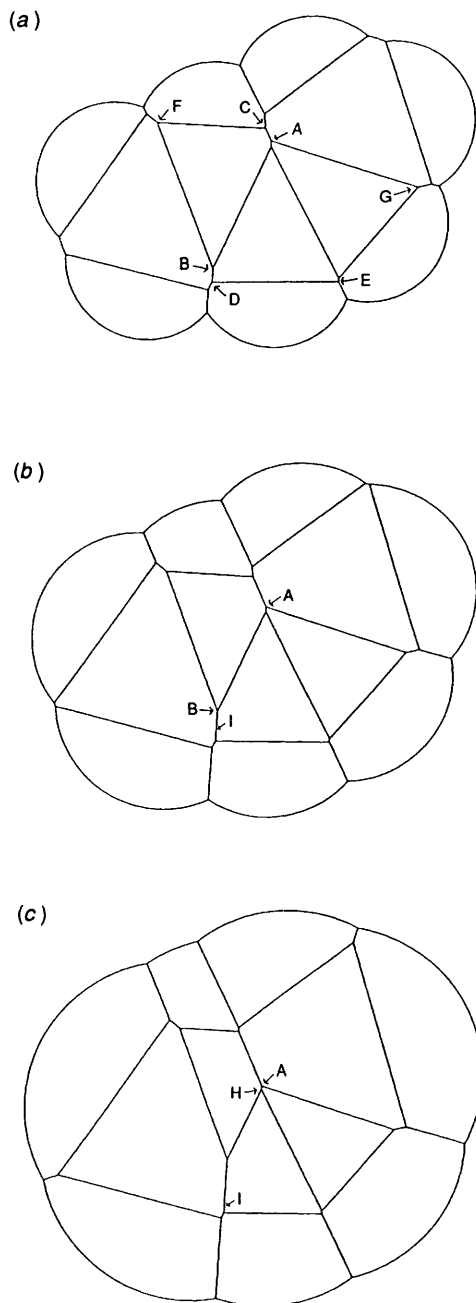


Figure 5. Ion-pair surfaces and associated HSE minima for the Li^+ , Cs^+ , and SS^+ ion pairs of S-pentadienyl^- . The terms used are defined in the headings to Figures 1 and 2. Since the anion is planar $\bar{\text{A}}$ lies directly below A . S-Pentadienyl^- , Li^+ [Figure 5(a)] (i) HMO charge distribution, minimum at $\text{A}, \bar{\text{A}}$, 129.9; local minima at $\text{B}, \bar{\text{B}}$, 122.0; no further local minima. (ii) CNDO-II charge distribution, minimum at $\text{A}, \bar{\text{A}}$, 118.9; local minima at $\text{C}, \bar{\text{C}}$, 118.6; $\text{D}, \bar{\text{D}}$, 117.7; $\text{E}, \bar{\text{E}}$, 106.7; $\text{F}, \bar{\text{F}}$, 104.0; $\text{G}, \bar{\text{G}}$, 100.3; no further local minima. S-Pentadienyl^- , Cs^+ [Figure 5(b)] HMO charge distribution, minimum at $\text{A}, \bar{\text{A}}$, 91.5; local minima at $\text{B}, \bar{\text{B}}$, 86.7; no further local minima. S-Pentadienyl^- , SS^+ [Figure 5(c)] HMO charge distribution, minimum at $\text{A}, \bar{\text{A}}$, 52.3; no local minima. S-Pentadienyl^- , 2Li^+ [Fig. 5(a)] HMO charge distribution, minimum at $\text{A}-\bar{\text{B}}$, $\bar{\text{A}}-\bar{\text{B}}$, 175.3; local minima not checked. S-Pentadienyl^- , 2Cs^+ [Figure 5(b)] HMO charge distribution, minimum at $\text{A}-\bar{\text{B}}$, $\bar{\text{A}}-\bar{\text{B}}$, 128.3; local minima not checked. S-Pentadienyl^- , 2SS^+ [Figure 5(c)] HMO charge distribution, minimum at $\text{H}-\bar{\text{H}}$, 76.8; local minima not checked. S-Pentadienyl^- , Li^+ , Cs^+ [Figures 5(a) and (b)] HMO charge distribution, minimum at A [Figure 5(a)]- $\bar{\text{I}}$ [Figure 5(b)], $\bar{\text{A}}-\bar{\text{I}}$, 155.7; local minima not checked. S-Pentadienyl^- , Li^+ , SS^+ [Figures 5(a) and (c)] HMO charge distribution, minimum at A [Figure 5(a)]- $\bar{\text{I}}$ [Figure 5(c)], $\bar{\text{A}}-\bar{\text{I}}$, 140.1; local minima not checked.

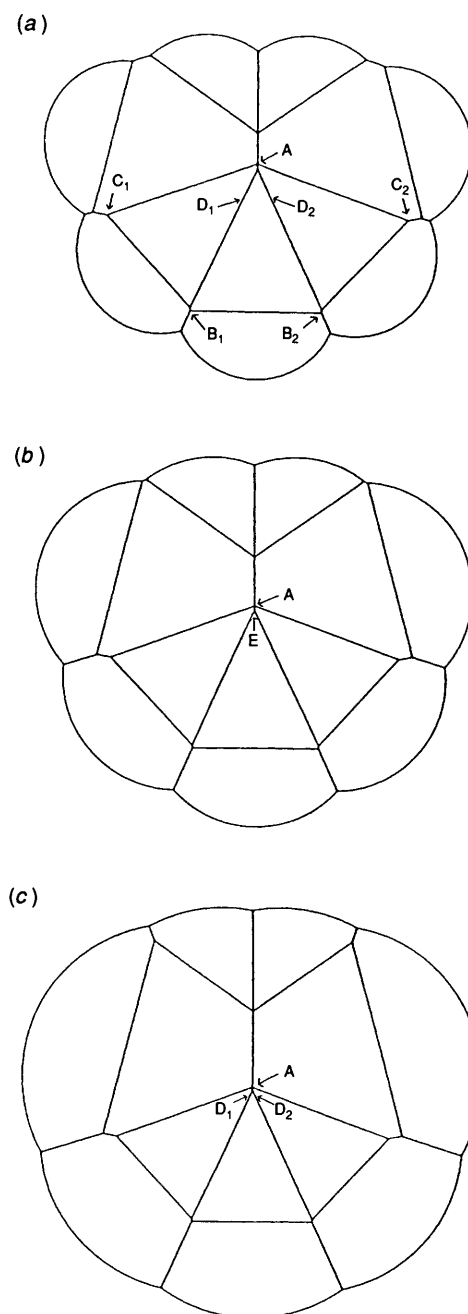


Figure 6. Ion-pair surfaces and associated HSE minima for the Li^+ , Cs^+ , and SS^+ ion pairs of U-pentadienyl^- . The terms used are defined in the headings to Figures 1 and 2. Since the anion is planar $\bar{\text{A}}$ lies directly below A . U-Pentadienyl^- , Li^+ [Figure 6(a)] (i) HMO charge distribution, minimum at $\text{A}, \bar{\text{A}}$, 145.7; no local minima. (ii) CNDO-II charge distribution, minimum at $\text{A}, \bar{\text{A}}$, 129.6; local minima at $\text{B}_1, \bar{\text{B}}_1$, $\text{B}_2, \bar{\text{B}}_2$, 107.3; $\text{C}_1, \bar{\text{C}}_1$, $\text{C}_2, \bar{\text{C}}_2$, 102.2; no further local minima. U-Pentadienyl^- , Cs^+ [Figure 6(b)] HMO charge distribution, minimum at $\text{A}, \bar{\text{A}}$, 97.8; no local minima. U-Pentadienyl^- , SS^+ [Figure 6(c)] HMO charge distribution, minimum at $\text{A}, \bar{\text{A}}$, 53.5; no local minima. U-Pentadienyl^- , 2Li^+ [Figure 6(a)] HMO charge distribution, minimum at $\text{A}-\bar{\text{D}}_1$, $\text{A}-\bar{\text{D}}_2$, $\bar{\text{A}}-\bar{\text{D}}_1$, $\bar{\text{A}}-\bar{\text{D}}_2$, 181.0; local minima not checked. U-Pentadienyl^- , 2Cs^+ [Figure 6(b)] HMO charge distribution, minimum at $\text{A}-\bar{\text{A}}$, 138.5; local minima not checked. U-Pentadienyl^- , 2SS^+ [Figure 6(c)] HMO charge distribution, minimum at $\text{A}-\bar{\text{A}}$, 79.2; no local minima. U-Pentadienyl^- , Li^+ , Cs^+ [Figures 6(a) and (b)] HMO charge distribution, minimum at A [Figure 6(a)]- $\bar{\text{E}}$ [Figure 6(b)], $\bar{\text{A}}-\bar{\text{E}}$, 167.8; local minima not checked. U-Pentadienyl^- , Li^+ , SS^+ [Figures 6(a) and (c)] HMO charge distribution, minimum at A [Figure 6(a)]- $\bar{\text{D}}_1$ [Figure 6(c)], $\text{A}-\bar{\text{D}}_2$, $\bar{\text{A}}-\bar{\text{D}}_1$, $\bar{\text{A}}-\bar{\text{D}}_2$, 154.5; local minima not checked.

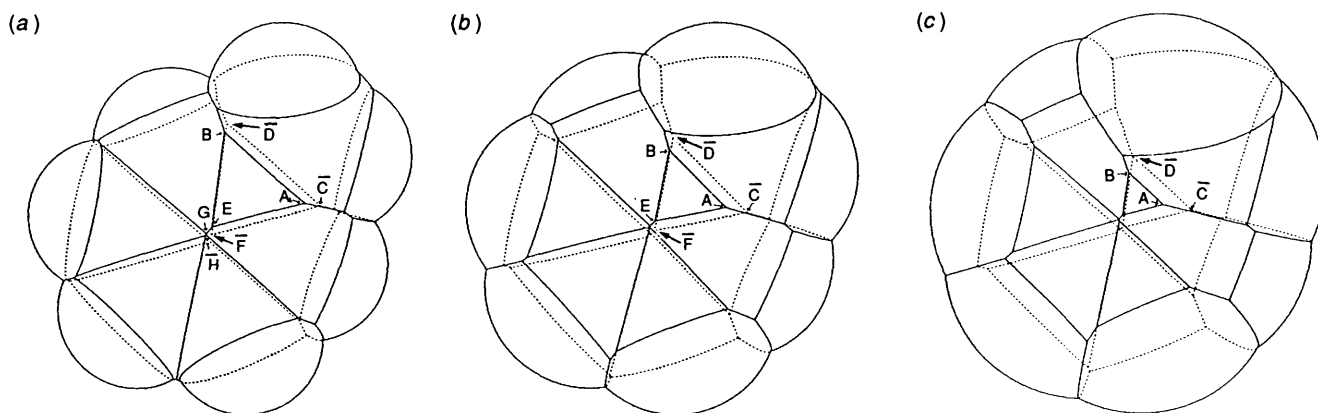
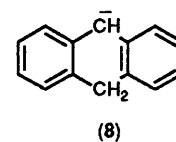
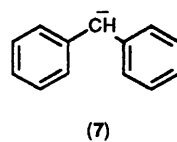


Figure 7. Ion-pair surfaces and associated HSE minima for the Li^+ , Cs^+ , and SS^+ ion pairs of benzyl $^-$. The terms used are defined in the headings to Figures 1 and 2. The anion geometry used is non-planar (ref. 41). Discontinuities on the lower surface are encoded by the use of dashed lines and cation bonding sites by the letters with a bar. Benzyl $^-$, Li^+ [Figure 7(a)] (i) HMO charge distribution, minimum at A,B (equal in energy), 130.4; local minima at C, 129.4; D, 129.3; E, 120.3; F, 118.1; no further local minima. (ii) STO-3G *ab initio* charge distribution, minimum at G, 128.1; local minima at H, 126.7; B, 120.9; A, 120.3, C, 118.8; D, 117.4; no further local minima. Benzyl $^-$, Cs^+ [Figure 7(b)] HMO charge distribution, minimum at A,B, 91.5; local minima at C,D, 90.4; E,F, 86.5; no further local minima. Benzyl $^-$, SS^+ [Figure 7(c)] HMO charge distribution, minimum at A,B, 52.3; local minima at C,D, 51.7; no further local minima. Benzyl $^-$, 2Li^+ [Figure 7(a)] HMO charge distribution, minimum at B-C, 182.8; local minima not checked. Benzyl $^-$, 2Cs^+ [Figure 7(b)] HMO charge distribution, minimum at B-C, 131.8; local minima not checked. Benzyl $^-$, 2SS^+ [Figure 7(c)] HMO charge distribution, minimum at B-C, 77.0; local minima not checked. Benzyl $^-$, Li^+ , Cs^+ [Figures 7(a) and (b)] HMO charge distribution, minimum at A [Figure 7(a)]-D [Figure 7(b)], 160.1; local minima not checked. Benzyl $^-$, Li^+ , SS^+ [Figures 7(a) and (c)] HMO charge distribution, minimum at A [Figure 7(a)]-D [Figure 7(c)], 141.8.

The Benzhydryl Anion.—Despite many studies of the chemistry of the lithium salts of the benzhydryl anion (7) and the related anion (8) derived from dihydroanthracene there is remarkably little reliable structural information. An X-ray crystal structure of the 12-crown-4 complex of the lithium salt of anion (7) shows a planar benzhydryl unit which is taken by the authors to be typical of the free anion.⁵⁷ MNDO MO calculations on the free anion⁴² suggest, however, that the phenyl rings should be twisted in a conrotatory sense by 25° and that the degree of twisting of the rings is enhanced on pairing with Li^+ . The anion (8), on the other hand, is constrained to remain close to planar. MNDO calculations on the lithium salt of this anion suggest that the cation will adopt a position over the central ring [more or less equivalent to position A in Figure 8(a)].⁴⁸ For the HSE calculations we used a geometry for the benzhydryl anion which is almost planar.⁵⁸ The resultant ion-pair structures are shown in Figure 8. For the 1:1 benzhydryl-lithium ion pair the minimum is found at position A [(Figure 8(a))] which is equivalent to that predicted by MO calculations and is a site which is equivalent to the η^3 site in benzyl-lithium but with respect to both benzene rings. This site where the cation bridges the α -carbon and two *ortho*-carbons is superior to sites B and C where only the α -carbon and one *ortho*-carbon are bridged. Sites over the benzene rings D and E are much less favoured. In the triple ions cation/cation repulsion normally prevents occupation of both sites A and A except when both cations are of the solvent-separated type.

The Trityl Anion.—Several X-ray crystallographic studies have been made of group 1 metal salts of the trityl anion, $\{\text{Ph}_3\text{C}, \text{Li}, \text{Me}_2\text{NCH}_2\text{CH}_2\text{NMe}_2\}$,⁵⁹ $\{\text{Ph}_3\text{C}, \text{Na}, \text{Me}_2\text{NCH}_2\text{CH}_2\text{NMe}_2\}$,⁶⁰ $\{\text{Ph}_3\text{C}, \text{Li}, (12\text{-crown-4})_2\}$,⁵⁷ and $\{\text{Ph}_3\text{C}, \text{Li}, \text{Et}_2\text{O}\}$.⁶¹ In all of these the trityl ligand adopts a propeller shaped conformation with unequal degrees of rotation about the three rings (between 20 and 45°). In the sodium salt and in the lithium-crown ether complex the central carbon is planar but in the other two lithium salts it is slightly pyramidal (0.12 Å out of the plane containing the three adjacent carbons).^{59,61} In the crown ether complex⁵⁷ there are no close contacts between the lithium and trityl anion but, in the three



other structures, the two closest contacts are to the central carbon and the first carbon (*n*-carbon) of the least twisted phenyl ring, with between one and three further contacts to an *ortho*-carbon of this ring or the *n*- or *ortho*-carbons of another ring [i.e., more or less along the lines A-C or D-F in Figure 9(a)]. For the HSE calculations the geometry of trityl determined by Brooks and Stucky⁵⁹ (with a slightly pyramidal central carbon) was adopted. The resultant ion-pair surfaces are found in Figure 9. For the trityl-lithium the area of the energy surface near the central carbon is very flat and even after careful inspection of contour diagrams it was difficult to be absolutely certain that all of the local minima found by the 'automatic search' routines were genuine. However, the absolute minimum is close to the X-ray crystallographic structure.

The 1,3-Diphenylallyl Anion.—In most solvents the predominant geometry of the 1,3-diphenylallyl anion is *trans,trans*⁶² but small amounts of the *cis,trans*-isomer can also be detected.⁶³ The third possible isomer, *cis,cis*, is only found on conformationally rigid derivatives.⁶⁴ In crystalline [1,3-diphenylallyl, Li, Et_2O] $_\infty$ ⁶⁵ the diphenylallyl unit is planar, *trans,trans*, and has a geometry close to that predicted by CNDO-II MO calculations on the free anion.^{64,66} The lithium counterion is in an η^3 site bridging the two α -carbons [close to position A in Figure 10(a)] whilst the bridging diethyl ether ligands complete an 'infinite' chain. CNDO-II calculations on *trans,trans*-1,3-diphenylallyl anion predict this type of η^3 site for the absolute minimum with local energy minima for the lithium in η^3 α -carbon/*ortho*-carbon bridging sites [close to sites B and E in Figure 10(a)] and further local minima over the benzene rings [close to sites F in Figure 10(a)].⁶⁴ CNDO-II MO calculations on *cis,trans*- and *cis,cis*-1,3-diphenylallyl-lithium give similar results.

For the HSE calculations the geometries used for the three isomers were those that have been partially optimised for the

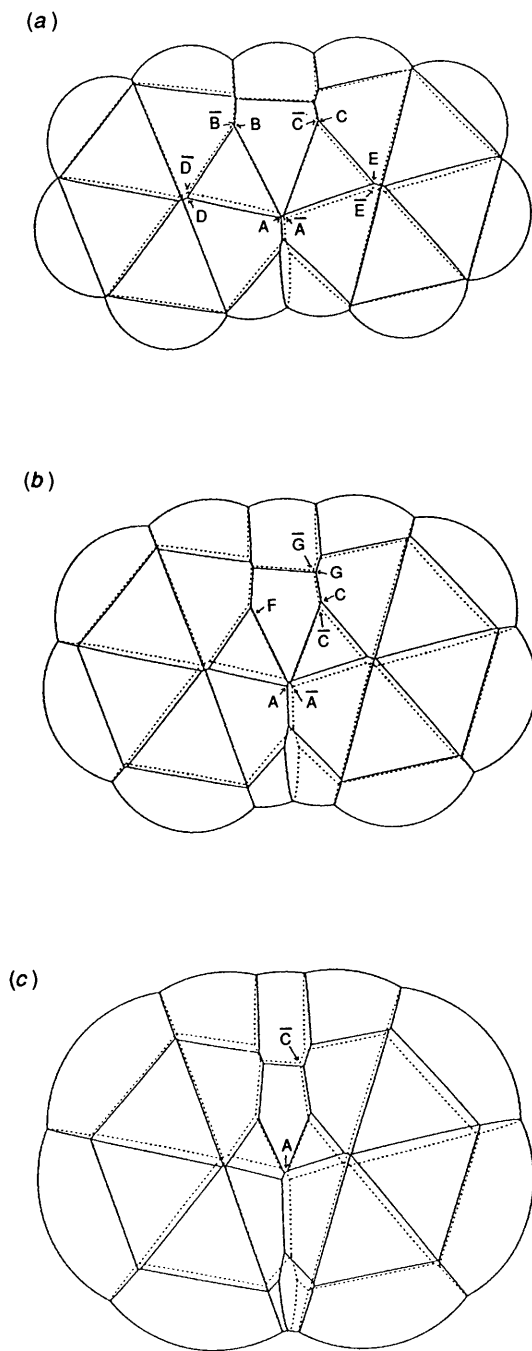


Figure 8. Ion-pair surfaces and associated HSE minima for the Li^+ , Cs^+ , and SS^+ ion pairs of benzhydryl $^-$. The terms used are defined in the headings to Figures 1, 2, and 7. Since the geometry chosen (ref. 58) is almost planar \bar{A} lies almost directly below A. The difference in energy for paired sites of this type is very small (<0.4) and only the values for the better minimum of each pair is given. HMO charge distributions were used in all cases. *Benzhydryl $^-$, Li $^+$* [Figure 8(a)] minimum at A, \bar{A} , 122.2; local minima at B, \bar{B} , 112.7; C, \bar{C} , 112.6; D, \bar{D} , 101.3; E, \bar{E} , 100.8; no further local minima. *Benzhydryl $^-$, Cs $^+$* [Figure 8(b)] minimum at A, \bar{A} , 87.4; no local minima. *Benzhydryl $^-$, SS $^+$* [Figure 8(c)] minimum at A, \bar{A} , 51.2; no local minima. *Benzhydryl $^-$, 2Li $^+$* [Figure 8(a)] minimum at B, \bar{A} , \bar{B} -A, 158.0; local minima not checked. *Benzhydryl $^-$, 2Cs $^+$* [Figure 8(b)] minimum at A-F, \bar{A} -F, 120.0; local minima not checked. *Benzhydryl $^-$, 2SS $^+$* [Figure 8(c)] minimum at A- \bar{A} , 74.6; local minima not checked. *Benzhydryl $^-$, Li $^+$, Cs $^+$* [Figures 8(a) and (b)] minimum at A [Figure 8(a)]- \bar{C} [Figure 8(b)], \bar{A} -G, 143.3; local minima not checked. *Benzhydryl $^-$, Li $^+$, SS $^+$* [Figures 8(a) and (c)] minimum at A [Figure 8(a)]- \bar{C} [Figure 8(c)], \bar{A} -C, 131.2; local minima not checked.

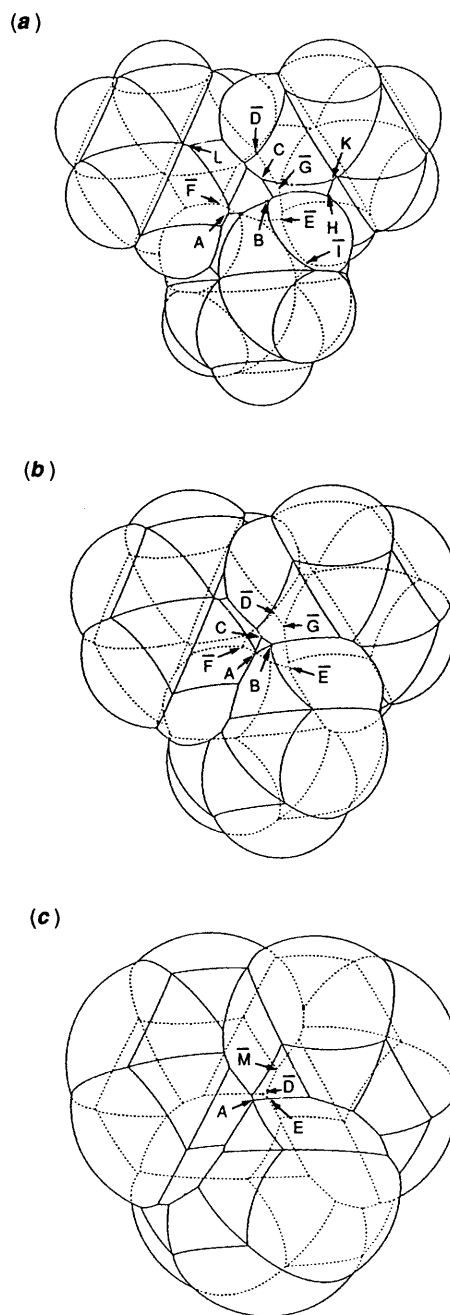


Figure 9. Ion-pair surfaces and associated HSE minima for the Li^+ , Cs^+ , and SS^+ ion pairs of trityl $^-$. The terms used are defined in the headings to Figures 1, 2 and 7. *Trityl $^-$, Li $^+$* [Figure 9(a)] (i) HMO charge distribution, minimum at A, 111.8; minima at B, 111.1; C, 111.0; D, \bar{E} , 108.7; F, 107.9; G, 107.0; H, 96.7; I, 95.6; no further local minima. (ii) CNDO-II charge distribution; local minimum at C, 95.8; local minima at A, \bar{D} , 93.8; E, 92.4; F, 92.1; K, 86.4; L, 84.8; no further local minima. *Trityl $^-$, Cs $^+$* [Figure 9(b)] HMO charge distribution, minimum at A, 83.4; local minima at B, C 83.3; E, 80.6; further local minima not checked. *Trityl $^-$, SS $^+$* [Figure 9(c)] HMO charge distribution, minimum at \bar{D} , 49.0; local minimum at A 48.8; no further local minima. *Trityl $^-$, 2Li $^+$* [Figure 9(a)] HMO charge distribution, minimum at A-G, 145.3; local minimum not checked. *Trityl $^-$, 2Cs $^+$* [Figure 9(b)] HMO charge distribution, minimum at C-E, 114.7; local minima not checked. *Trityl $^-$, 2SS $^+$* [Figure 9(c)] HMO charge distribution, minimum at A- \bar{E} , 71.4; local minima not checked. *Trityl $^-$, Li $^+$, Cs $^+$* [Figures 9(a) and (b)] minimum at A [Figure 9(a)]-G [Figure 9(b)], 133.0; local minima not checked. *Trityl $^-$, Li $^+$, SS $^+$* [Figures 9(a) and (c)] minimum at A [Figure 9(a)]- \bar{M} [Figure 9(c)], 121.0; local minima not checked.

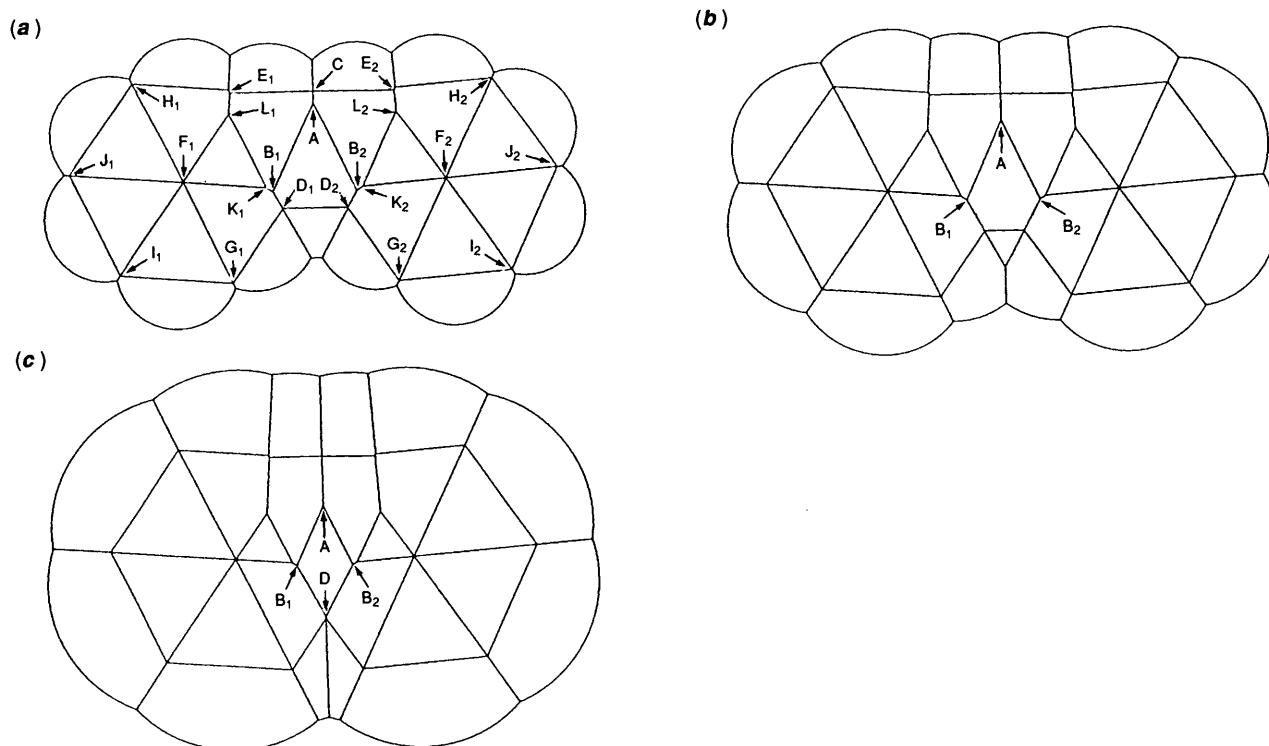


Figure 10. Ion-pair surfaces and associated HSE minima for the Li^+ , Cs^+ and SS^+ ion pairs of (E, E) -1,3-diphenylallyl $^-$. The terms used are defined in the headings to Figures 1 and 2. Since the geometry chosen is planar \bar{A} lies directly below A. (E, E) -1,3-Diphenylallyl $^-$, Li^+ [Figure 10(a)] (i) HMO charge distribution, minimum at \bar{A}, \bar{A} , 113.8; local minima at $\bar{B}_1, \bar{B}_2, \bar{B}_1, \bar{B}_2$, 106.6; no further local minima. (ii) CNDO-II charge distribution, minimum at \bar{C}, \bar{C} , 101.9; local minima at $\bar{B}_1, \bar{B}_2, \bar{B}_1, \bar{B}_2$, 90.5; $\bar{D}_1, \bar{D}_2, \bar{D}_1, \bar{D}_2$, 90.0; $\bar{E}_1, \bar{E}_2, \bar{E}_1, \bar{E}_2$, 89.7; $\bar{F}_1, \bar{F}_2, \bar{F}_1, \bar{F}_2$, 77.1; $\bar{G}_1, \bar{G}_2, \bar{G}_1, \bar{G}_2$, 72.4; $\bar{H}_1, \bar{H}_2, \bar{H}_1, \bar{H}_2$, 68.9; $\bar{I}_1, \bar{I}_2, \bar{I}_1, \bar{I}_2$, 64.6; $\bar{J}_1, \bar{J}_2, \bar{J}_1, \bar{J}_2$, 63.9; no further local minima. (E, E) -1,3-Diphenylallyl $^-$, Cs^+ [Figure 10(b)] HMO charge distribution, minimum at \bar{A}, \bar{A} , 82.4; local minima at $\bar{B}_1, \bar{B}_2, \bar{B}_1, \bar{B}_2$, 80.1; no further local minima. (E, E) -1,3-Diphenylallyl $^-$, SS^+ [Figure 10(c)] HMO charge distribution, minimum at \bar{A}, \bar{A} , 49.5; local minima at $\bar{B}_1, \bar{B}_2, \bar{B}_1, \bar{B}_2$, 49.5; no further local minima. (E, E) -1,3-Diphenylallyl $^-$, 2Li^+ [Figure 10(a)] HMO charge distribution, minimum at $\bar{K}_1, \bar{L}_2, \bar{K}_2, \bar{L}_1, \bar{K}_1, \bar{L}_2, \bar{K}_2, \bar{L}_1$, 145.0; local minima not checked. (E, E) -1,3-Diphenylallyl $^-$, 2Cs^+ [Figure 10(b)] HMO charge distribution, minimum at $\bar{B}_1, \bar{B}_2, \bar{B}_1, \bar{B}_2$, 112.5; local minima not checked. (E, E) -1,3-Diphenylallyl $^-$, 2SS^+ [Figure 10(c)] HMO charge distribution, minimum at $\bar{A}, \bar{D}, \bar{A}, \bar{D}$, 71.7; local minima not checked. (E, E) -1,3-Diphenylallyl $^-$, Li^+ , Cs^+ [Figures 10(a) and (b)] HMO charge distribution, minimum at A [Figure 10(a)]- \bar{B}_1 [Figure 10(b)], $\bar{A}, \bar{B}_2, \bar{A}, \bar{B}_1, \bar{A}, \bar{B}_2$, 132.5; local minima not checked. (E, E) -1,3-Diphenylallyl $^-$, Li^+ , SS^+ [Figures 10(a) and (c)] HMO charge distribution, minimum at A [Figure 10(a)]- \bar{D} [Figure 10(c)] \bar{A}, \bar{D} , 123.0; local minima not checked.

free anions at the CNDO-II level.^{64,66} In the case of the *trans,trans*-isomer this is very close to that found in the crystal structure of the lithium diethyl ether complex.⁶⁵ The results of these calculations are shown in Figures 10–12. The HSE calculations for the 1:1 lithium ion pairs [Figures 10(a), 11(a), 12(a)] give results which are in good agreement with MO calculations so far as the positions and orderings of the energy minima are concerned. Perhaps the only significant difference is that the HSE calculation for the *cis,cis*-isomer finds additional minima over the benzene rings and in α -carbon/*ortho*-carbon bridging sites. As is normal in almost all these systems, as the size of the counterion increases $\text{Li}^+ \rightarrow \text{Cs}^+ \rightarrow \text{SS}^+$ the position of the absolute minimum remains essentially the same but the energy surface becomes flatter and local minima are progressively lost.

The Cyclopentadienyl Anion.—Various SCF-MO calculations on cyclopentadienyl-lithium^{67,68} suggest that the metal ion should be centrally placed (η^5) over the cyclopentadienyl ring. There is a very slight bending of the hydrogens away from the metal ion (~ 2 – 3° out of plane) which is thought to be induced by the electrostatic influence of the metal ion.⁶⁸ The central η^5 site is found in crystalline (cyclopentadienide, Na, $\text{Me}_2\text{NCH}_2\text{CH}_2\text{NMe}_2$)⁶⁹ and in various other X-ray crystallographic studies of lithium⁷⁰ and sodium salts⁷¹ of cyclopentadienide derivatives. The ^7Li NMR chemical shift for cyclopentadienyl-

lithium has been interpreted as evidence that the Li^+ is located over the ring.⁷²

HSE calculations agree with the MO and X-ray crystallographic results in predicting a central η^5 site for the counterion in 1:1 ion pairs. This is also predicted to be the favoured site in cyclopentadienyl $^-$, M_1^+ , M_2^+ triple ions (Figure 13).

The Indenyl Anion.—The X-ray crystallographic structure of [indenyl, Li, $\text{Me}_2\text{NCH}_2\text{CH}_2\text{NMe}_2$] has been known since 1975.⁷³ It shows the lithium more or less in the η^5 site, central over the five-membered ring [equivalent to site A in Figure 14(a)]. On the other hand [indenyl, Na, $\text{Me}_2\text{NCH}_2\text{CH}_2\text{NMe}_2$] $_\infty$ has an 'infinite' chain structure in which each sodium bridges two indenyl ligands occupying sites that are η^1 relative to one and η^2 relative to the other.⁷⁴ The reasons for these differences have been discussed by Schleyer who points out that MNDO calculations on indenyl-lithium reveal two bonding sites; the absolute minimum with the lithium over the five-membered ring and a local minimum with the lithium over the six-membered ring.⁷⁴ ^1H NMR,⁷⁵ ^7Li NMR,⁷² and ^{13}C NMR⁷⁶ studies of the lithium,^{72,74,75} sodium,^{72,74,75} and potassium⁷⁴ salts in ether solvents have all been interpreted as supporting a structure in which the cation is placed over the five-membered ring although ^1H NMR work on indenyl-lithium was at one time interpreted as supporting a position over the six-membered ring.^{74,77} In some transition metal complexes it is known that

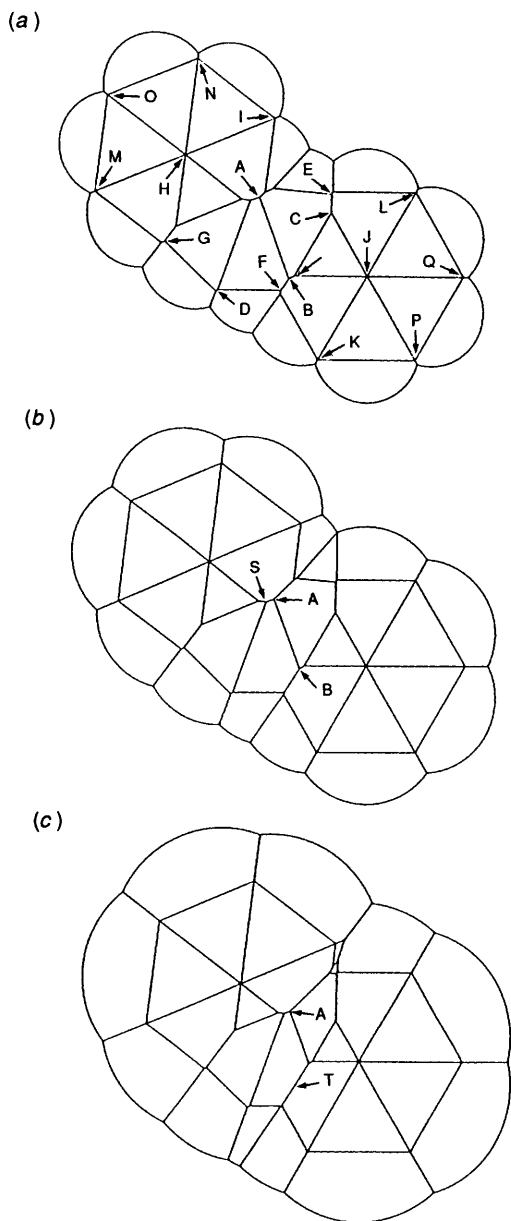


Figure 11. Ion-pair surfaces and associated HSE minima for the Li^+ , Cs^+ , and SS^+ ion pairs of (Z,E) -1,3-diphenylallyl $^-$. The terms used are defined in the headings to Figures 1 and 2. Since the geometry chosen is planar \bar{A} lies directly below A. (Z,E) -1,3-Diphenylallyl $^-$, Li^+ [Figure 11(a)] (i) HMO charge distribution, minimum at A, \bar{A} , 118.5; local minima at B, \bar{B} , 105.9; C, \bar{C} , 100.2; no further local minima. (ii) CNDO-II charge distribution, minima at A, \bar{A} , 99.2; local minima at D, \bar{D} , 92.2; E, \bar{E} , 91.1; B, \bar{B} , 90.8; F, \bar{F} , 90.2; G, \bar{G} , 89.1; H, \bar{H} , 98.8; I, \bar{I} , 77.5; J, \bar{J} , 77.2; K, \bar{K} , 71.3; L, \bar{L} , 69.6; M, \bar{M} , 69.1; N, \bar{N} , 66.5; O, \bar{O} , 64.9; P, \bar{P} , 64.4; Q, \bar{Q} , 64.0; no further local minima. (Z,E) -1,3-Diphenylallyl $^-$, Cs^+ [Figure 11(b)] HMO charge distribution, minimum at A, \bar{A} , 85.4; local minimum at B, \bar{B} , 79.5; no further local minima. (Z,E) -1,3-Diphenylallyl $^-$, SS^+ [Figure 11(c)] HMO charge distribution, minimum at A, \bar{A} , 50.4; no local minima. (Z,E) -1,3-Diphenylallyl $^-$, 2Li^+ [Figure 11(a)] HMO charge distribution, minimum at A, \bar{A} , 148.6; local minima not checked. (Z,E) -1,3-Diphenylallyl $^-$, 2Cs^+ [Figure 11(b)] HMO charge distribution, minimum at S, \bar{S} , 114.9; local minima not checked. (Z,E) -1,3-Diphenylallyl $^-$, 2SS^+ [Figure 11(c)] HMO charge distribution, minimum at A, \bar{A} , 73.0; local minima not checked. (Z,E) -1,3-Diphenylallyl $^-$, Li^+ , Cs^+ [Figures 11(a) and (b)] HMO charge distribution, minimum at A [Figure 11(a)]– \bar{B} [Figure 11(b)], \bar{A} – \bar{B} , 136.5; local minima not checked. (Z,E) -1,3-Diphenylallyl $^-$, Li^+ , SS^+ [Figures 11(a) and (c)] HMO charge distribution, minimum at A [Figure 11(a)]– \bar{T} [Figure 11(c)], \bar{A} – \bar{T} , 126.3; local minima not checked.

both η^5 and η^6 sites can be occupied and the interconversion of these species has been studied.⁷⁸

For the HSE calculations Stucky's geometry for indenyl was used. For 1:1 complexes HSE calculations on the lithium salt give the absolute minimum over the five-membered ring and a local minimum over the six-membered ring, but for larger counterions only the η^5 site is found. In triple ions the calculations suggest that the η^5 sites are again the ones to be occupied.

The Fluorenyl Anion.—The X-ray crystallographic structure of {fluorenyl, Li, N[CH₂CH₂]₃N} shows the lithium in a site analogous to that in benzyl-lithium in which it bridges the CH position of the five-membered ring and the nearest CH position of the six-membered ring.⁷⁹ This site is predicted to be a local minimum by MNDO MO calculations but these predict that the absolute minimum is at the η^5 site where the lithium is over the middle of the five-membered ring.⁴² Some support for the idea that this η^5 site is actually the site occupied by the lithium in fluorenyl-lithium solution comes from ⁷Li NMR⁸⁰ and ¹³C NMR work.⁸¹ The η^5 site is also that occupied by the potassium in (fluorenyl, K, Me₂NCH₂CH₂NMe₂) although in this case the X-ray crystal structure shows the cation bridging two fluorenyl ligands.⁸²

For the HSE calculations the fluorenyl geometry was taken from that of Stucky.⁷⁹ For 1:1 complexes the HSE calculations suggest that the η^5 site (Figure 15, site A) is the absolute minimum. In the case of fluorenyl-lithium local minima are also found over the six-membered ring [Figure 15(a), site B] but, although the energy surface is very flat in the region where the lithium is located in {fluorenyl, Li, N[CH₂CH₂]₃N} no local minima are found.

Carbocation Ion Pairs.—The first evidence for ion pairs in organic reactions came from carbocation rather than carbanion chemistry. The presence of ion-pair intermediates were suggested in order to explain the stereochemistry of some S_N1 solvolyses⁸³ and the later studies of Winstein established that in some of these solvolyses both contact and solvent-separated ion pairs were important.⁸⁴ Sneen and others have also suggested that some 'S_N2' reactions involve rate-determining attack of a nucleophile on a preformed carbocation ion-pair.⁸⁵ Despite the undoubted importance of ion pairs in carbocation chemistry, depictions of the structures of such ion pairs remain rudimentary. For the odd alternant systems discussed in this paper (allyl, pentadienyl, benzyl, benzhydryl, trityl, and 1,3-diphenylallyl) the HMO charge distribution in the cation is the mirror image of that in the anion. Hence the results of an HSE calculation will be the same and the calculations we have performed can also be used as a first-order guide to carbocation ion-pair structures (although it should be noted that the smallest X⁻ counterions, e.g. Cl⁻, are similar to Cs⁺ in radius and none, of course, are as small as Li⁺). Hence from the HSE standpoint an allyl cation ion-pair will be analogous to allyl⁻, Cs⁺ or allyl⁻, SS⁺ [Figure 2(b) and 2(c)] with the anion symmetrically bridging the two CH₂⁺ groups. Such structures (13) have been proposed for solvent-separated ion pairs but the proposal that the enantiomeric halides (9) and (10) give unsymmetrical contact ion pairs (11) and (12) seems suspect unless these 'ion pairs' really have a substantial degree of covalent bonding.⁸⁵ Similarly the ion pairs formed by solvolysis of benzyl halides are normally depicted with the counterion centrally placed. On the basis that these structures should be analogous to Figure 7(b) and 7(c) it seems more realistic to suggest that the counterion would bridge the α -carbon and *ortho*-carbon. Similarly in reactions where a charged nucleophile attacks a preformed carbocation ion-pair the HSE calculations on carbanion triplets may give a guide to the structures involved.⁸⁵

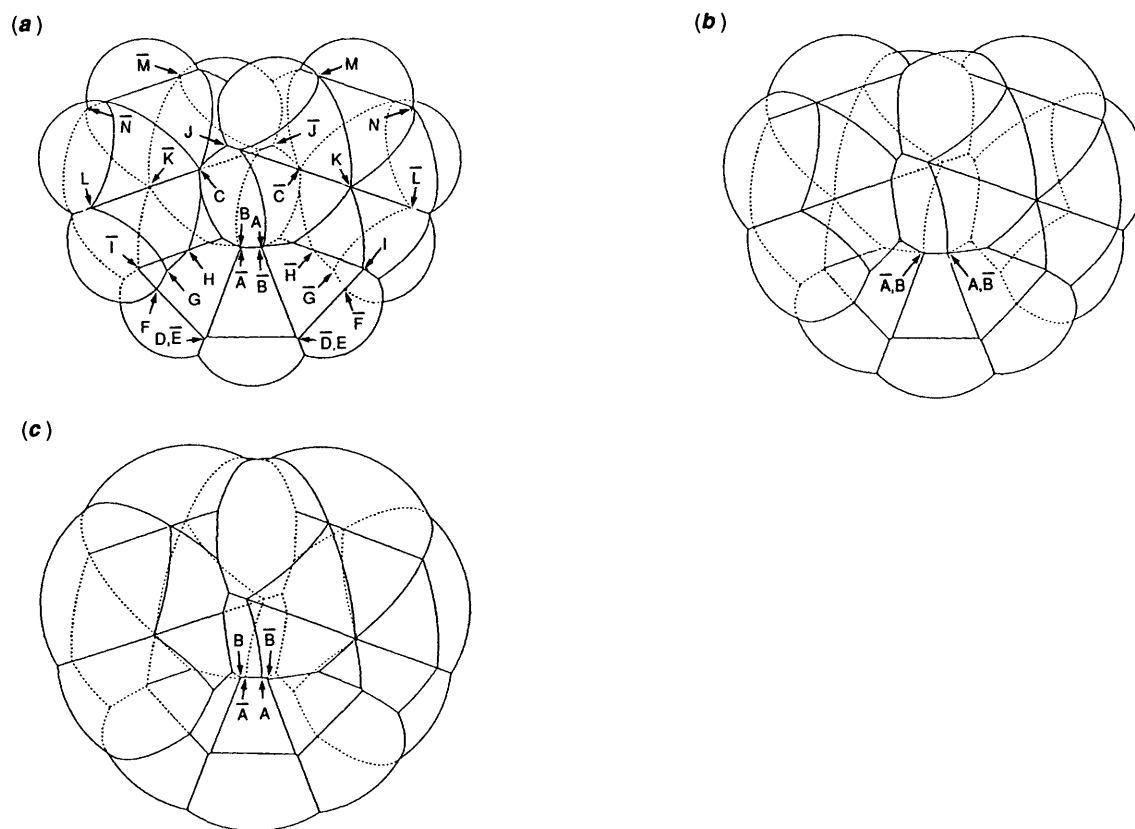


Figure 12. Ion-pair surfaces and associated HSE minima for the Li^+ , Cs^+ and SS^+ ion pairs of (Z,Z) -1,3-diphenylallyl $^-$. The terms used are defined in the headings to Figures 1, 2, and 7. \bar{A} is related to A via a C_2 rotational axis. (Z,Z) -1,3-Diphenylallyl $^-$, Li^+ [Figure 12(a)] (i) HMO charge distribution, minimum at A, \bar{A} , 118.9; local minima at B, \bar{B} , 118.5; C, \bar{C} , 99.5; no further local minima (ii) CNDO-II charge distribution, minimum at B, \bar{B} , 94.8; local minima at A, \bar{A} , 94.5; D, \bar{D} , E, \bar{E} , 92.4; F, \bar{F} , 91.1; G, \bar{G} , 90.9; H, \bar{H} , 90.5; I, \bar{I} , 89.3; C, \bar{C} , 86.1; J, \bar{J} , 84.0; K, \bar{K} , 80.4; L, \bar{L} , 72.9; M, \bar{M} , 71.8; N, \bar{N} , 68.9; no further local minima. (Z,Z) -1,3-Diphenylallyl $^-$, Cs^+ [Figure 12(b)] HMO charge distribution, minimum at A, \bar{A} , B, \bar{B} , 84.8, no local minima. (Z,Z) -1,3-Diphenylallyl $^-$, SS^+ [Figure 12(c)] HMO charge distribution, minimum at B, \bar{B} , 49.8; local minima at A, \bar{A} , 49.7; no local minima. (Z,Z) -1,3-Diphenylallyl $^-$, 2Li^+ [Figure 12(a)] HMO charge distribution, minimum at A, \bar{A} , 152.6; local minima not checked. (Z,Z) -1,3-Diphenylallyl $^-$, 2Cs^+ [Figure 12(b)] HMO charge distribution, minimum at B, \bar{B} , 118.8; local minima not checked. (Z,Z) -1,3-Diphenylallyl $^-$, 2SS^+ [Figure 12(c)] HMO charge distribution, minimum at B, \bar{B} , 72.7; local minima not checked. (Z,Z) -1,3-Diphenylallyl $^-$, Li^+ , Cs^+ [Figures 12(a) and (b)] HMO charge distribution, minimum at A [Figure 12(a)]- \bar{A} [Figure 12(b)] 140.2; local minima not checked. (Z,Z) -1,3-Diphenylallyl $^-$, Li^+ , SS^+ [Figures 12(a) and (c)] HMO charge distribution, minimum at A [Figure 12(a)]- \bar{A} [Figure 12(c)] 128.0; local minima not checked.

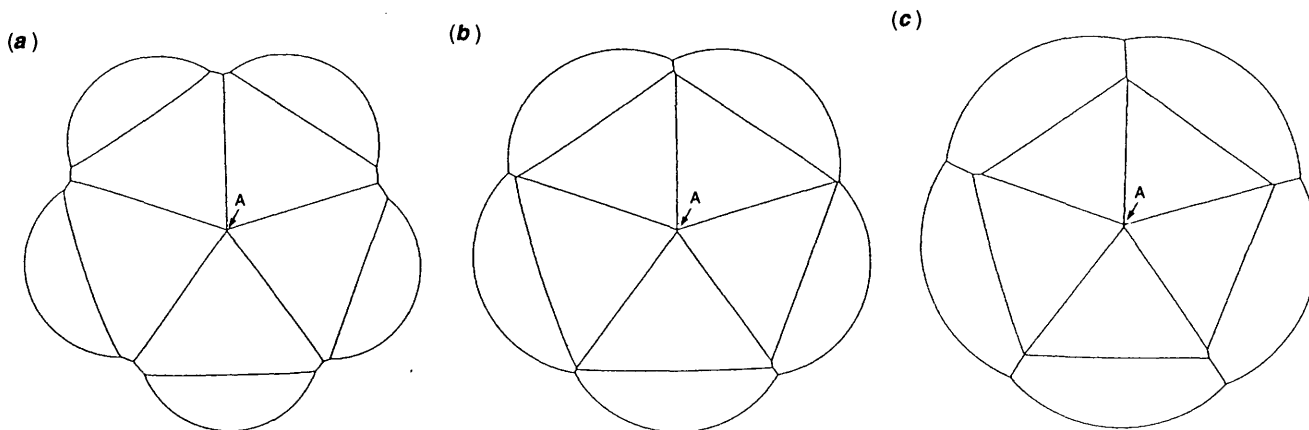


Figure 13. Ion-pair surfaces and associated HSE minima for the Li^+ , Cs^+ , and SS^+ ion pairs of cyclopentadienyl $^-$. The terms used are defined in the headings to Figures 1 and 2. HMO charge distributions are used in each case. The anion is planar and \bar{A} lies directly below A . Cyclopentadienyl $^-$, Li^+ [Figure 13(a)] minimum at A, \bar{A} , 146.1; no local minima. Cyclopentadienyl $^-$, Cs^+ [Figure 13(b)] minimum at A, \bar{A} , 97.9; no local minima. Cyclopentadienyl $^-$, SS^+ [Figure 13(c)] minimum at A, \bar{A} , 53.5; no local minima. Cyclopentadienyl $^-$, 2Li^+ [Figure 13(a)] minimum at A, \bar{A} , 206.7; local minima not checked. Cyclopentadienyl $^-$, 2Cs^+ [Figure 13(b)] minimum at A, \bar{A} , 143.6; local minima not checked. Cyclopentadienyl $^-$, 2SS^+ [Figure 13(c)] minimum at A, \bar{A} , 79.8; local minima not checked. Cyclopentadienyl $^-$, Li^+ , Cs^+ [Figures 13(a) and (b)] minimum at A , [Figure 13(a)]- \bar{A} [Figure 13(b)], 179.2; local minima not checked. Cyclopentadienyl $^-$, Li^+ , SS^+ [Figures 13(a) and (c)] minimum at A (Figure 13a)- \bar{A} [Figure 13(c)], 158.4; local minima not checked.

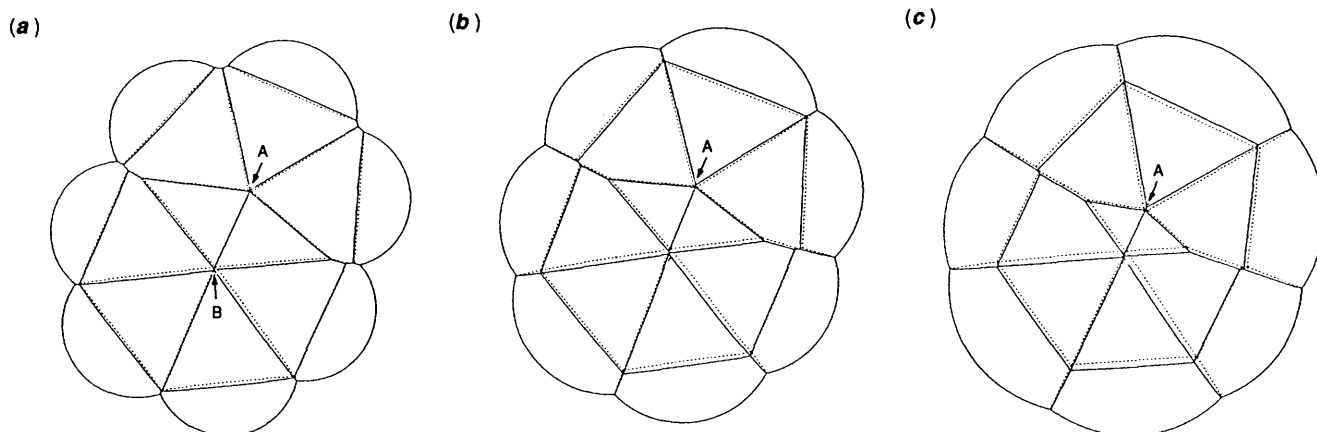


Figure 14. Ion-pair surfaces and associated HSE minima for the Li^+ , Cs^+ , and SS^+ ion pairs of indenyl $^-$. The terms used are defined in the headings to Figures 1, 2, and 7. The anion geometry chosen is almost planar. \bar{A} lies almost directly below A and as in the case of benzhydryl the energies of positions on the top and bottom surface are so close that they are not listed separately, just the lower energy partner of the pair. Indenyl $^-$, Li^+ [Figure 14(a)] (i) HMO charge distribution, minimum at A, \bar{A} , 135.8; local minimum at B, \bar{B} , 116.9; no further local minima. (ii) STO-3G *ab initio* MO charge distribution, minimum at A, \bar{A} , 126.2; local minima at B, \bar{B} , 124.2; no further local minima. Indenyl $^-$, Cs^+ [Figure 14(b)] HMO charge distribution, minimum at A, \bar{A} , 93.5; no local minima. Indenyl $^-$, SS^+ [Figure 14(c)] HMO charge distribution, minimum at A, \bar{A} , 52.6; no local minima. Indenyl $^-$, 2Li^+ [Figure 14(a)] HMO charge distribution, minimum at A- \bar{A} , 185.8; local minima not checked. Indenyl $^-$, 2Cs^+ [Figure 14(b)] HMO charge distribution, minimum at A- \bar{A} , 134.8; local minima not checked. Indenyl $^-$, 2SS^+ [Figure 14(c)] HMO charge distribution, minimum at A- \bar{A} , 77.9; local minima not checked. Indenyl $^-$, Li^+ , Cs^+ [Figures 14(a) and (b)] HMO charge distribution, minimum at A [Figure 14(a)]- \bar{A} [Figure 14(b)], 164.4; local minima not checked. Indenyl $^-$, Li^+ , SS^+ [Figures 14(a) and (c)] HMO charge distribution, minimum at A [Figure 14(a)]- \bar{A} [Figure 14(c)], 147.1; local minima not checked.

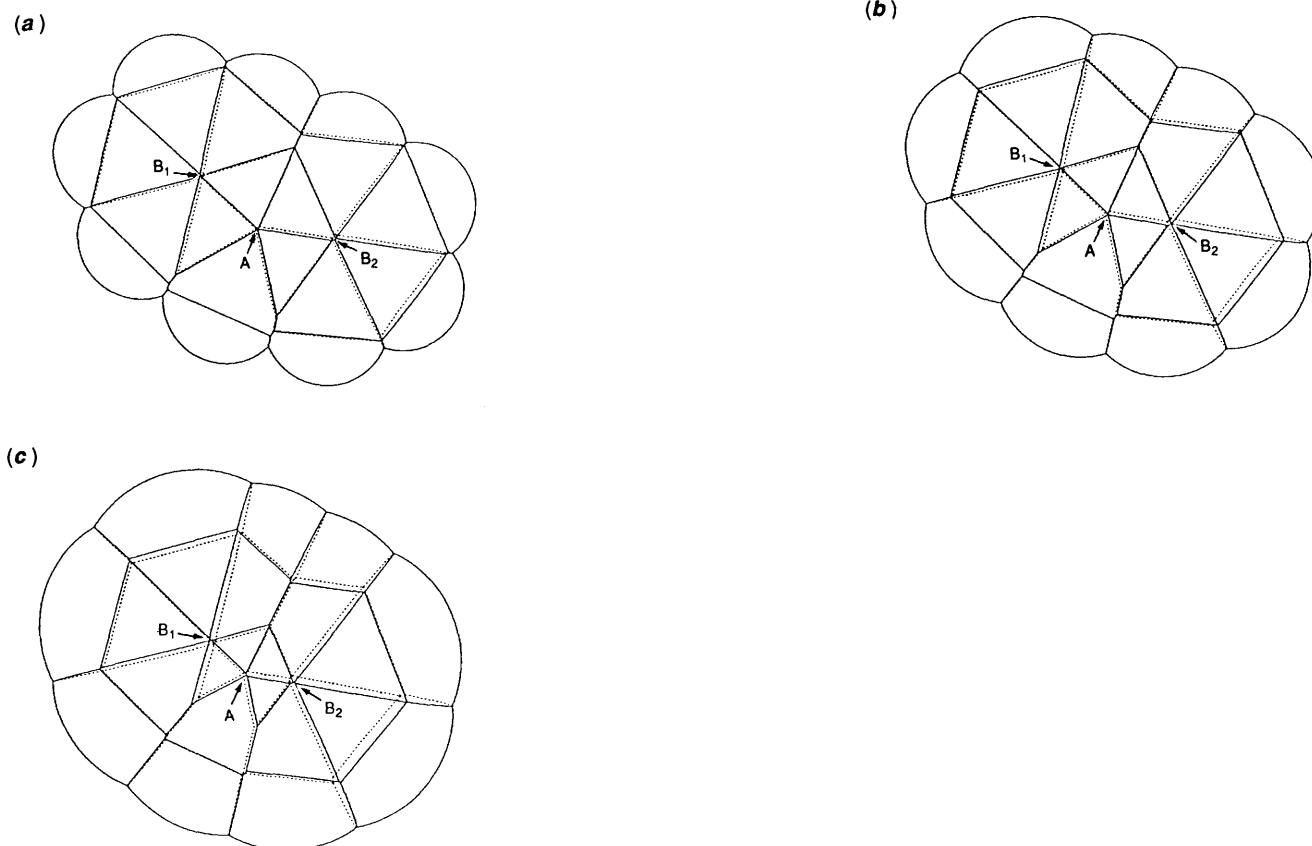
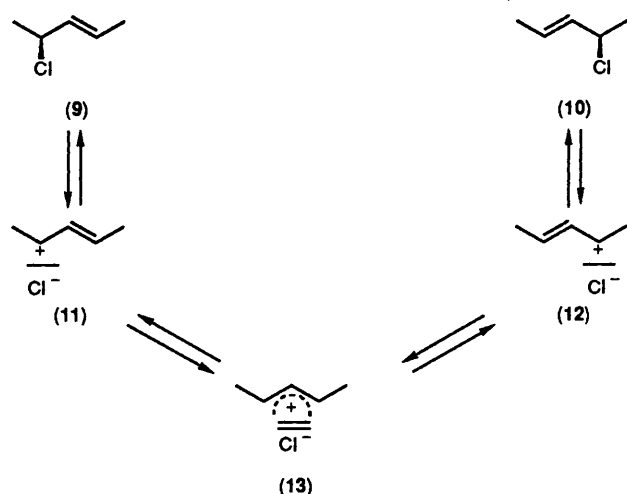


Figure 15. Ion-pair surfaces and associated HSE minima for the Li^+ , Cs^+ , and SS^+ ion pairs of fluorenyl $^-$. The terms used are defined in the headings to Figures 1, 2, and 7. The anion geometry chosen is almost planar. \bar{A} lies almost directly below A and the energies for positions on the top and bottom surface are so close that they are not listed separately, just the lower energy partner in each pair. HMO charge distributions are used in each case. Fluorenyl $^-$, Li^+ [Figure 15(a)] minimum at A, \bar{A} , 127.0; local minima at B $_1$, B $_2$, \bar{B}_1 , \bar{B}_2 , 108.5; no further local minima. Fluorenyl $^-$, Cs^+ [Figure 15(b)] minimum at A, \bar{A} , 89.8; no local minima. Fluorenyl $^-$, SS^+ [Figure 15(c)] minimum at A, \bar{A} , 51.8; no local minima. Fluorenyl $^-$, 2Li^+ [Figure 15(a)] minimum at A- \bar{A} , 167.6; local minima not checked. Fluorenyl $^-$, 2Cs^+ [Figure 15(b)] minimum at A- \bar{A} , 127.2; local minima not checked. Fluorenyl $^-$, 2SS^+ [Figure 15(c)] minimum at A- \bar{A} , 76.2; local minima not checked. Fluorenyl $^-$, Li^+ , Cs^+ [Figures 15(a) and (b)] minimum at A [Figure 15(a)]- \bar{A} [Figure 15(b)], \bar{A} -A, 151.6; local minima not checked. Fluorenyl $^-$, Li^+ , SS^+ [Figures 15(a) and (c)] minimum at A [Figure 15(a)]- \bar{A} [Figure 15(c)], \bar{A} -A 137.3; local minima not checked.



Scheme. Anionotropic rearrangement of optically active 2-chloropent-3-ene (9) and (10) involving contact-ion-pair intermediates (11) and (12) and a solvent-separated-ion-pair intermediate (13).

Carbanion Ion Pairs: General Conclusions.—In this paper the predictions of HSE calculations, mostly for 1:1 organolithium ion pairs, have been compared with known crystal structures and with structures predicted by MO methods. It can be argued that none of these approaches gives a reliable guide to the structures of these ion pairs in solution but in most cases all three agree and in such cases it would, indeed, be remarkable if the solution structure were something different. The good agreement between the HSE results and those obtained by other methods show that it is incorrect to claim that 'simple electrostatics cannot explain the structures of ion pairs of delocalised anions'⁵ and rather that simple electrostatics gives a good first-order guide to such structures. Since the method works well for organolithiums it seems reasonable to argue that the structures predicted for Cs⁺ and SS⁺ ion pairs are probably correct. These calculations suggest that as the size of the counterion increases the energy surface becomes flatter, and local minima are lost, but the absolute minimum-energy position of the counterion remains unchanged. The W-pentadienyl ion is the only exception which we have found. Cases like that of the pyrazinyl radical anion ion-pairs, where the site occupied by the counterion is thought to change with the size of the cation, must be seen as exceptional.⁸⁶ Although it seems that these HSE calculations reliably locate all of the significant minima on these ion pair energy surfaces one problem with the method is the large number of high-energy local minima found when non-HMO MO charge distributions are employed. These may not be significant. Another problem is whether some of the structures predicted for the triple ions are significant. There are no data against which these can be checked. Although such structural predictions are, perhaps, best regarded as provisional the general conclusions with respect to these triple ions seem sound. In particular that cation/cation repulsion prevents most triple ions R⁻, 2Li⁺ being 'doubled up' versions of R⁻, Li⁺ and results in R⁻, 2Li⁺ being unstable relative to R⁻, Li⁺, SS⁺ and often relative to R⁻, 2SS⁺.¹

Acknowledgements

We thank the SERC for financial assistance.

References

- Part 10, R. J. Bushby and H. L. Steel, preceding paper.
- R. J. Bushby and H. L. Steel, *J. Organomet. Chem.*, 1987, **336**, C25 and references therein.
- (a) W. N. Setzer and P. von R. Schleyer, *Adv. Organomet. Chem.*, 1985, **24**, 353; (b) C. Shade and P. von R. Schleyer, *ibid.*, 1987, **27**, 169 and references therein.
- R. F. W. Bader and P. J. MacDougall, *J. Am. Chem. Soc.*, 1985, **107**, 6788.
- G. Stucky, *Adv. Chem. Ser.*, 1974, **130**, 56.
- R. J. Bushby and A. S. Patterson, *J. Organomet. Chem.*, 1977, **132**, 163.
- A. J. Kos and P. von R. Schleyer, *J. Am. Chem. Soc.*, 1980, **102**, 7928.
- Preliminary communication of part of this work: R. J. Bushby and M. P. Tytko, *J. Organomet. Chem.*, 1984, **270**, 265.
- R. J. Bushby and H. L. Steel, following paper.
- R. J. Bushby and G. J. Ferber, *J. Chem. Soc., Chem. Commun.*, 1973, **407**; *J. Chem. Soc., Perkin Trans. 2*, 1976, 1683, 1688, 1695.
- J. E. Norlander and J. D. Roberts, *J. Am. Chem. Soc.*, 1959, **81**, 1769.
- C. S. Johnson, M. A. Weiner, J. S. Waugh, and D. Seyferth, *J. Am. Chem. Soc.*, 1961, **83**, 1306.
- D. A. Hutchinson, K. R. Beck, R. A. Benkeser, and J. B. Grutzner, *J. Am. Chem. Soc.*, 1973, **95**, 7075.
- M. Schlosser and M. Stähle, *Angew. Chem., Int. Ed. Engl.*, 1980, **19**, 487.
- M. Saunders, L. Telkowski, and M. R. Kates, *J. Am. Chem. Soc.*, 1977, **99**, 8070; J. W. Faller, H. H. Murray, and M. Saunders, *ibid.*, 1980, **102**, 2306.
- C. Prévost, M. Gaudemar, L. Miginiac, F. Bardone-Gaudemar, and M. Andrac, *Bull. Soc. Chim. Fr.*, 1959, 679.
- M. Marsch, K. Harms, W. Massa, and G. Boche, *Angew. Chem., Int. Ed. Engl.*, 1987, **26**, 696.
- S. Brownstein, S. Bywater, and D. J. Worsfold, *J. Organomet. Chem.*, 1980, **199**, 1.
- W. Neugebauer and P. von R. Schleyer, *J. Organomet. Chem.*, 1980, **198**, C1.
- M. Stähle and M. Schlosser, *J. Organomet. Chem.*, 1981, **220**, 277.
- W. R. Winchester, W. Bauer, and P. von R. Schleyer, *J. Chem. Soc., Chem. Commun.*, 1987, 177.
- P. West and R. Waack, *J. Am. Chem. Soc.*, 1967, **89**, 4395; P. West, J. I. Purmort, and S. V. McKinley, *ibid.*, 1968, **90**, 797; P. West, R. Waack, and J. I. Purmort, *ibid.*, 1970, **92**, 840.
- G. R. Brubaker and P. Beak, *J. Organomet. Chem.*, 1977, **136**, 147.
- H. Köster and E. Weiss, *Chem. Ber.*, 1982, **115**, 3422.
- U. Schümann, E. Weiss, H. Dietrich, and W. Mahdi, *J. Organomet. Chem.*, 1987, **322**, 299.
- N. Hertkorn, F. H. Köhler, G. Müller, and G. Reber, *Angew. Chem., Int. Ed. Engl.*, 1986, **25**, 468.
- D. Seebach, T. Maetzke, R. K. Haynes, M. N. Paddon-Row, and S. S. Wong, *Helv. Chim. Acta*, 1988, **71**, 299.
- J. F. Sebastian, J. R. Grunwell, and B. Hsu, *J. Organomet. Chem.*, 1974, **78**, C1; E. R. Tidwell and B. R. Russell, *ibid.*, 1974, **80**, 175; G. B. Erusalimskii and V. A. Korner, *Zh. Org. Khim.*, 1984, **20**, 2028.
- T. Clark, E. D. Jemmis, P. von R. Schleyer, J. S. Binkley, and J. A. Pople, *J. Organomet. Chem.*, 1978, **150**, 1; G. Decher and G. Boche, *ibid.*, 1983, **259**, 31; T. Clark, C. Rhode, and P. von R. Schleyer, *Organometallics*, 1983, **2**, 1344.
- E. J. Lanpher, *J. Am. Chem. Soc.*, 1957, **79**, 5578.
- D. T. Clark and D. R. Armstrong, *Theor. Chim. Acta*, 1969, **14**, 370; J. R. Grunwell and J. F. Sebastian, *Tetrahedron*, 1971, **27**, 4387; A. Y. Meyer and M. Chrinovitzky, *J. Mol. Struct.*, 1972, **12**, 157; A. Atkinson, A. C. Hopkinson, and E. Lee-Ruff, *Tetrahedron*, 1974, **30**, 2023; G. I. Mackay, M. H. Lien, A. C. Hopkinson, and D. K. Bohme, *Can. J. Chem.*, 1978, **56**, 131.
- H. Yasuda, Y. Ohnuma, M. Yamauchi, H. Tani, and A. Nakamura, *Bull. Chem. Soc. Jpn.*, 1979, **52**, 2036; H. Yasuda, M. Yamauchi, and A. Nakamura, *J. Organomet. Chem.*, 1980, **202**, C1; H. Yasuda, M. Yamauchi, A. Nakamura, and Y. Ohnuma, *Bull. Chem. Soc. Jpn.*, 1981, **54**, 1481.
- R. Hoffmann and R. A. Olofson, *J. Am. Chem. Soc.*, 1966, **88**, 943.
- L. M. Tolbert and A. Rajca, *J. Org. Chem.*, 1985, **50**, 4805; G. A. Olah, G. Asensio, H. Mayr, and P. von R. Schleyer, *J. Am. Chem. Soc.*, 1978, **100**, 4347.
- A. Bongini, G. Cainelli, G. Cardillo, P. Palmieri, and A. Umani-Rouchi, *J. Organomet. Chem.*, 1975, **92**, C1.
- H. Yasuda, M. Yamauchi, A. Nakamura, T. Sei, Y. Kai, N. Yasuoka, and N. Kasai, *Bull. Chem. Soc. Jpn.*, 1980, **53**, 1089, 1101.
- G. Fraenkel and M. P. Hallden-Abberton, *J. Am. Chem. Soc.*, 1981, **103**, 5657.
- J. F. Sebastian, B. Hsu, and J. R. Grunwell, *J. Organomet. Chem.*, 1976, **105**, 1.

- 39 H. Yasuda and A. Nakamura, *J. Organomet. Chem.*, 1985, **285**, 15.
- 40 M. Schlosser and M. Stähle, *Angew. Chem., Int. Ed. Engl.*, 1982, **21**, 145.
- 41 S. P. Patterman, I. L. Karle, and G. D. Stucky, *J. Am. Chem. Soc.*, 1970, **92**, 1150.
- 42 K. B. Lipkowitz, K. Uhegbu, A. M. Naylor, and R. Vance, *J. Comput. Chem.*, 1985, **6**, 662.
- 43 R. Waack, L. D. McKeever, and M. A. Doran, *Chem. Commun.*, 1969, 117.
- 44 R. R. Peoples and J. B. Grutzer, *J. Am. Chem. Soc.*, 1980, **102**, 4709.
- 45 L. M. Engelhardt, W.-P. Leung, C. L. Raston, P. Twiss, and A. H. White, *J. Chem. Soc., Dalton Trans.*, 1984, 321.
- 46 D. Colgan, R. I. Papasergio, C. L. Raston, and A. H. White, *J. Chem. Soc., Chem. Commun.*, 1984, 1708.
- 47 M. A. Beno, H. Hope, M. M. Olmstead, and P. P. Power, *Organometallics*, 1985, **4**, 2117.
- 48 R. Amstutz, J. D. Dunitz, and D. Seebach, *Angew. Chem., Int. Ed. Engl.*, 1981, **20**, 465.
- 49 B. Schubert and E. Weiss, *Chem. Ber.*, 1984, **117**, 366.
- 50 L. M. Engelhardt, R. I. Papasergio, C. L. Raston, and A. H. White, *J. Chem. Soc., Dalton Trans.*, 1984, 311.
- 51 M. F. Lappert, C. L. Raston, B. W. Skelton, and A. H. White, *J. Chem. Soc., Chem. Commun.*, 1982, 14.
- 52 G. Boche, G. Decher, H. Etzrodt, H. Dietrich, W. Mahdi, A. J. Kos, and P. von R. Schleyer, *J. Chem. Soc., Chem. Commun.*, 1984, 1493.
- 53 L. M. Engelhardt, W.-P. Leung, C. L. Raston, and A. H. White, *J. Chem. Soc., Dalton Trans.*, 1985, 337.
- 54 W.-P. Leung, C. L. Raston, B. W. Skelton, and A. H. White, *J. Chem. Soc., Dalton Trans.*, 1984, 1801.
- 55 A. J. Kos and P. von R. Schleyer as quoted in ref. 3(a).
- 56 A. Sygula and P. W. Rabideau, *J. Org. Chem.*, 1987, **52**, 3521.
- 57 M. M. Olmstead and P. P. Power, *J. Am. Chem. Soc.*, 1985, **107**, 2174.
- 58 Crystal Structure Search and Retrieval Program, Cambridge Crystallographic Data Centre.
- 59 J. J. Brooks and G. D. Stucky, *J. Am. Chem. Soc.*, 1972, **94**, 7333.
- 60 H. Köster and E. Weiss, *J. Organomet. Chem.*, 1979, **168**, 273.
- 61 R. A. Bartlett, H. V. R. Dias, and P. P. Power, *J. Organomet. Chem.*, 1988, **341**, 1.
- 62 J. W. Burley and R. N. Young, *J. Chem. Soc. B*, 1971, 1018; *J. Chem. Soc., Perkin Trans. 2*, 1972, 835, 1006.
- 63 R. J. Bushby, *J. Chem. Soc., Perkin Trans. 2*, 1980, 1419.
- 64 R. J. Bushby and A. S. Patterson, *J. Chem. Res.*, 1980, (S) 306; (M) 3801.
- 65 G. Boche, H. Etzrodt, M. Marsch, W. Massa, G. Bann, H. Dietrich, and W. Mahdi, *Angew. Chem., Int. Ed. Engl.*, 1986, **25**, 104.
- 66 R. J. Bushby, A. S. Patterson, G. J. Ferber, A. J. Duke, and G. H. Whitham, *J. Chem. Soc., Perkin Trans. 2*, 1978, 807.
- 67 R. Janoschek, G. Dierchsen, and H. Preuss, *Int. J. Quant. Chem. Symp.*, 1967, **1**, 205; S. Alexandratos, A. Streitwieser, and H. F. Schaefer, *J. Am. Chem. Soc.*, 1976, **98**, 7959; M. Lattman and A. H. Cowley, *Inorg. Chem.*, 1984, **23**, 241.
- 68 K. C. Waterman and A. Streitwieser, *J. Am. Chem. Soc.*, 1984, **106**, 3138.
- 69 T. Aoyagi, H. M. M. Shearer, K. Wade, and G. Whitehead, *J. Organomet. Chem.*, 1979, **175**, 21.
- 70 M. F. Lappert, A. Singh, L. M. Engelhardt, and A. H. White, *J. Organomet. Chem.*, 1984, **262**, 271; P. Jutzi, E. Schlüter, S. Pohl, and W. Saak, *Chem. Ber.*, 1985, **118**, 1959.
- 71 R. D. Rogers, J. L. Atwood, M. D. Rausch, D. W. Macomber, and W. P. Hart, *J. Organomet. Chem.*, 1982, **238**, 79; O. Mundt and G. Becker, *Zeit. Anorg. Allg. Chem.*, 1983, **496**, 58.
- 72 R. H. Cox, H. W. Terry, and L. W. Harrison, *J. Am. Chem. Soc.*, 1971, **93**, 3297.
- 73 W. E. Rhine and G. D. Stucky, *J. Am. Chem. Soc.*, 1975, **97**, 737.
- 74 C. Schade, P. von R. Schleyer, P. Gregory, H. Dietrich, and W. Mahdi, *J. Organomet. Chem.*, 1988, **341**, 19.
- 75 J. van der Kooij, N. H. Velthorst, and C. MacLean, *Chem. Phys. Lett.*, 1972, **12**, 596.
- 76 J. van der Giessen, C. Gooijer, C. MacLean, and N. H. Velthorst, *Chem. Phys. Lett.*, 1978, **55**, 33.
- 77 H. W. Vos, C. MacLean, and N. H. Velthorst, *J. Chem. Soc., Faraday Trans. 2*, 1976, **72**, 63.
- 78 T. A. Albright, P. Hofmann, R. Hoffmann, C. P. Lillya, and P. A. Dobosh, *J. Am. Chem. Soc.*, 1983, **105**, 3396; R. U. Kirss and P. M. Treichel, *ibid.*, 1986, **108**, 853.
- 79 J. J. Brooks, W. Rhine, and G. D. Stucky, *J. Am. Chem. Soc.*, 1972, **94**, 7339.
- 80 J. A. Dixon, P. A. Gwinner, and D. C. Lini, *J. Am. Chem. Soc.*, 1965, **87**, 1379.
- 81 U. Edlund, *Org. Magn. Reson.*, 1979, **12**, 661.
- 82 R. Zerger, W. Rhine, and G. D. Stucky, *J. Am. Chem. Soc.*, 1974, **96**, 5441.
- 83 W. von E. Doering and H. H. Zeiss, *J. Am. Chem. Soc.*, 1953, **75**, 4733.
- 84 S. Winstein, B. Appel, R. Baker, and A. Diaz, in 'Organic Reaction Mechanisms,' Chemical Society Special Publications, 1965, vol. 19.
- 85 R. A. Sneen and J. V. Carter, *J. Am. Chem. Soc.*, 1972, **94**, 6990; R. A. Sneen, *Acc. Chem. Res.*, 1973, **6**, 46.
- 86 P. Cremaschi, A. Gamba, and M. Simonetta, *Theor. Chim. Acta*, 1975, **40**, 303.

Paper 9/04103F

Received 25th September 1989

Accepted 7th February 1990